Lappeenranta-Lahti Univeristy of Technology
LUT School of Energy Systems
LUT Mechanical Engineering

Aleksandr Konovalov

MEASUREMENT OF THE REFLECTION COEFFICIENT OF THE CARBON-MANGANESE STEEL WIRE "OK AUTROD 12.64" USING FIBER LASER

Examiners: Professor Antti Salminen
PhD. Sc. (Tech.) Anna Unt

ABSTRACT

Lappeenranta University of Technology
LUT School of Energy Systems
LUT Mechanical Engineering

Aleksandr Konovalov

Measurement of the reflection coefficient of the carbon-manganese steel wire "OK Autrod 12.64" using fiber laser

Master's thesis

2019

63 pages, 45 figures, 13 tables

Examiners: Professor Antti Salminen
PhD. Sc. (Tech.) Anna Unt

Keywords: laser, wire, reflection, welding

In the literature review, the areas in which welding and additive laser technologies are applied using filler wire are examined. The relevance of study is proven by analytics of the data from the Scopus website. Some of the registration and modeling techniques of the working zone are described and compared to each other. A comparative review of benefits of using wire against powder in case of welding processes is done.

The experimental part explored methods for detecting the direction and power of the fiber laser radiation that is reflected from a wire. Through the analytic approach, the patterns which have the strongest affect on the characteristic of the reflected radiation and its magnitude is revealed. The obtained data are compared with the previous researcher's studies and the corresponding conclusions is made.

ACKNOWLEDGEMENTS

Thanks to the Flying Spaghetti Monster for creating the universe, me, my mind and for saving people from unscientific nonsense. Ramen.

Aleksandr Konovalov
Lappeenranta 3.11.2019

TABLE OF CONTENTS

LIST OF SYMBOLS AND ABBREVIATIONS

A	Absorption coefficient
d	Beam diameter [m]
P	Laser power [W]
q	Power density [W/m^2]
S	Size of an irradiation area [m^2]
π	Mathematical constant

3D	3-dimensional
AM	Additive Manufacturing
CO_2	Carbon dioxide
DED	Directed Energy Deposition
HAZ	Heat-affected zone
HLAW	Hybrid Laser-Arc Welding
Nd:YAG	Neodymium-doped Yttrium Aluminum Garnet
MIG	Metal Inert Gas
PBF	Powder Bed Fusion
PM	Parent Metal
TIG	Tungsten Inert Gas
WFR	Wire Feed Rate
WI	Weld Interface
WM	Welded Metal

1 INTRODUCTION

The topic of wire-based welding and Additive Manufacturing (AM) processes is very actual. An analysis of articles uploaded to the Scopus scientific database was carried out. For keywords, titles and a brief description, a search was made and it was found that the number of articles on laser- AM and welding processes (figure 1, 2) is increasing; it means that interest in wire-based systems is growing.

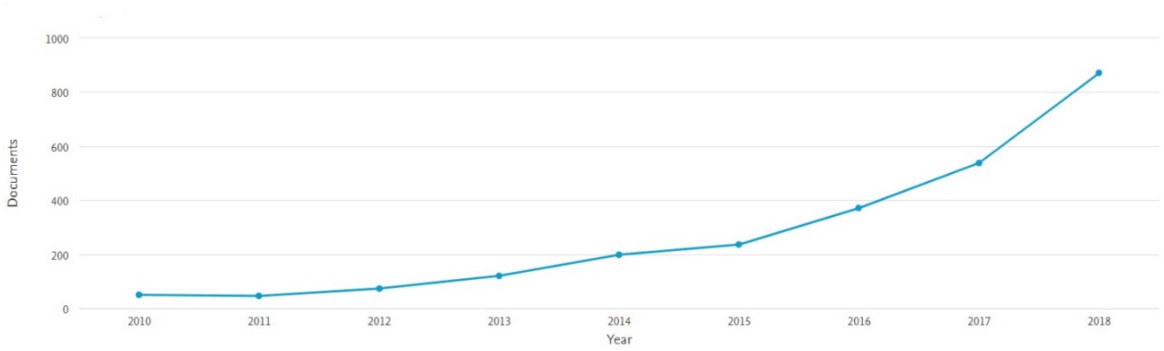

Figure 1. Analysis of the number of articles in Scopus for the search "wire AND laser AND welding" from the period from 2010 to 2018.

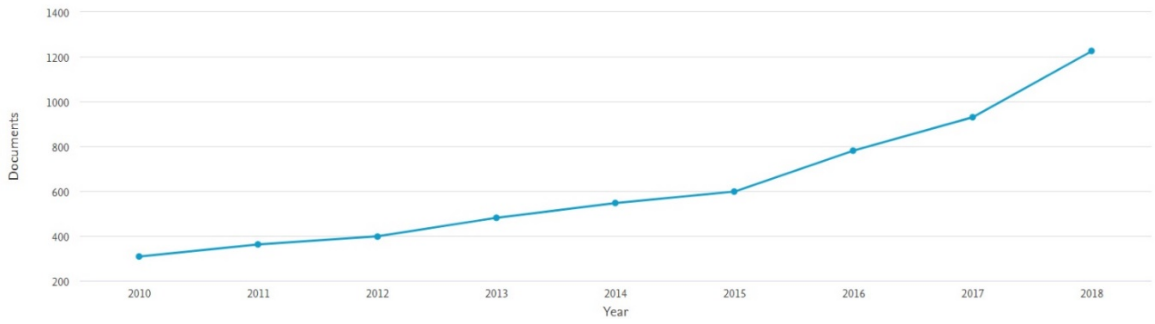

Figure 2. Analysis of the number of articles in Scopus for the search "wire AND laser AND additive manufacturing" from the period from 2010 to 2018.

The most important research interest has been studying the proper control of parameters in laser welding and AM. When it comes to wire-based additive manufacturing, it is important to know the proportions of energy absorbed and reflected from wire. Up to date, only a few investigations on process phenomena have been published, however understanding the process dynamics is of critical importance for process development. The reflection

phenomena taking place when using a Carbon dioxide (CO_2) laser as an energy source has been described by Salminen [1] and Arata et. al [2], however other complex studies on this topic were not found. In recent decade, high power solid state lasers have been replacing CO_2 lasers in many applications because of lower operating costs, flexible beam delivery and mobility. In addition, the near infrared wavelength of disk and fiber lasers (~ 1070 nm) has better absorption in metallic materials than radiation of CO_2 lasers (10 600 nm), meaning that larger fraction of energy applied is used in the process.

Motivation of current research work is to measure the reflection and find the reflection coefficient for the surface of carbon-manganese steel using fiber laser. Characterizing the reflection phenomena taking place during melting of wire has high scientific novelty and has not been previously explored, yet is especially relevant to further development of 3-dimensional (3D) printing technologies. Additive manufacturing with wire as a base material has certain similarities with laser welding and powder based AM processes. Literature review includes relevant studies from both fields to obtain a comprehensive summary of the topic.

Current thesis has theoretical and practical significance as gathered data can be applied in real manufacturing applications and results are valuable for further research dealing with process development of metal AM. Experimental part describes analytical approach to measuring data in different set-up's conditions. Modern detectors were used to determine the location of the reflected light and measuring it.

2 WELDING

Nowadays, each manufacturing industry anyway uses welded parts for different tasks. It gives higher power density and deeper penetration (figure 3) than traditional welding approaches and can be applied even in vacuum in comparing with plasma and arc welding. Also a deposition rate bigger in laser welding. It can work with a big range of materials and as with thin as thick sections. Robotization and automation are easier to realize. Also a big benefit is that laser welding can be applied in any position. All that are a reason why through years this technique is applied more and more.

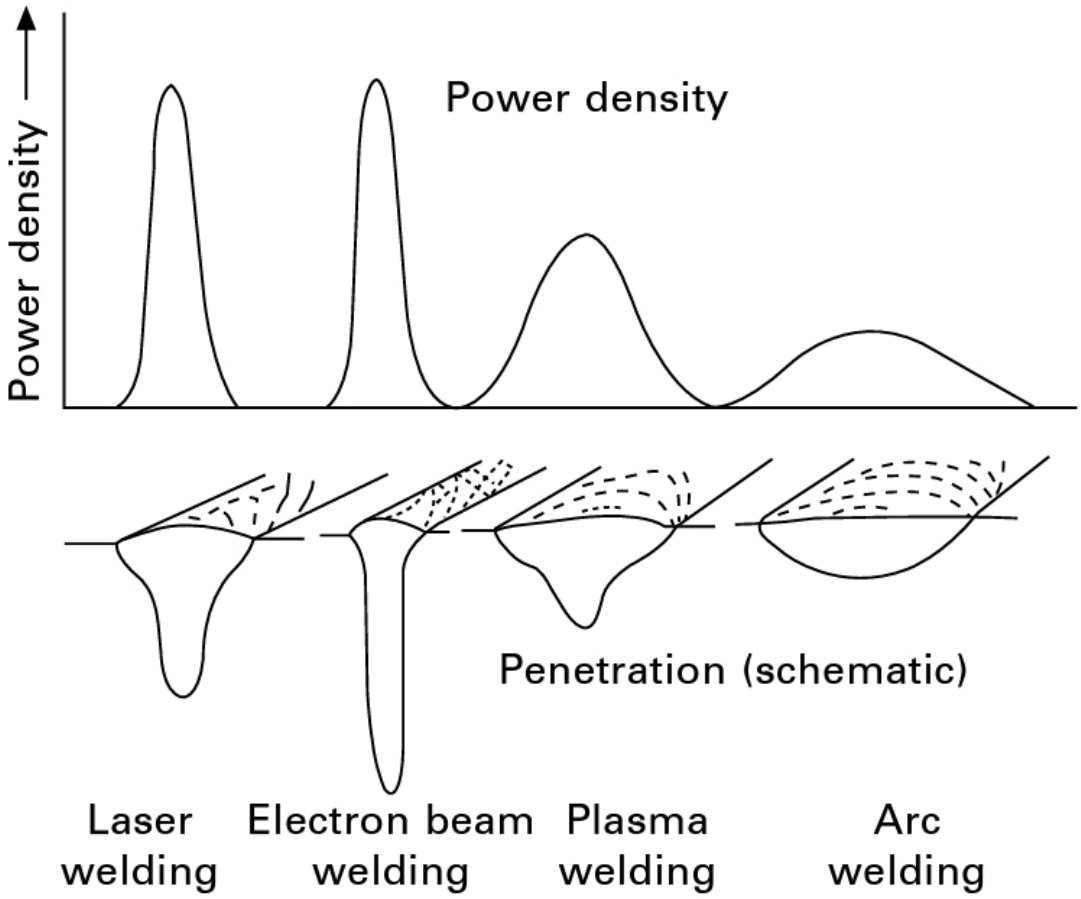

Figure 3. Power densities for typical welding heat sources, and geometry of weld beads obtained at respective densities [3].

2.1 Twin-beam laser welding technology

Laser welding process by itself has many advantages such as little Heat-affected zone (HAZ) in compare with other welding processes, high accuracy, tiny weld joint and quite deep

penetration. Unfortunately, it also has list of restraints in case of setting single-beam set-up. There are restrictions like a source power, beam width and others condition that depend on properties of the laser source. Dual-beam technique helps to overstep these limitations, as second beam is used simultaneously with the first one, thereby improving the process stability (figure 4). Another benefit of using this approach is possibility to increase the power applied to work piece. It is easy to calculate this meaning as it is just a sum of independent power characteristic of each source [4].

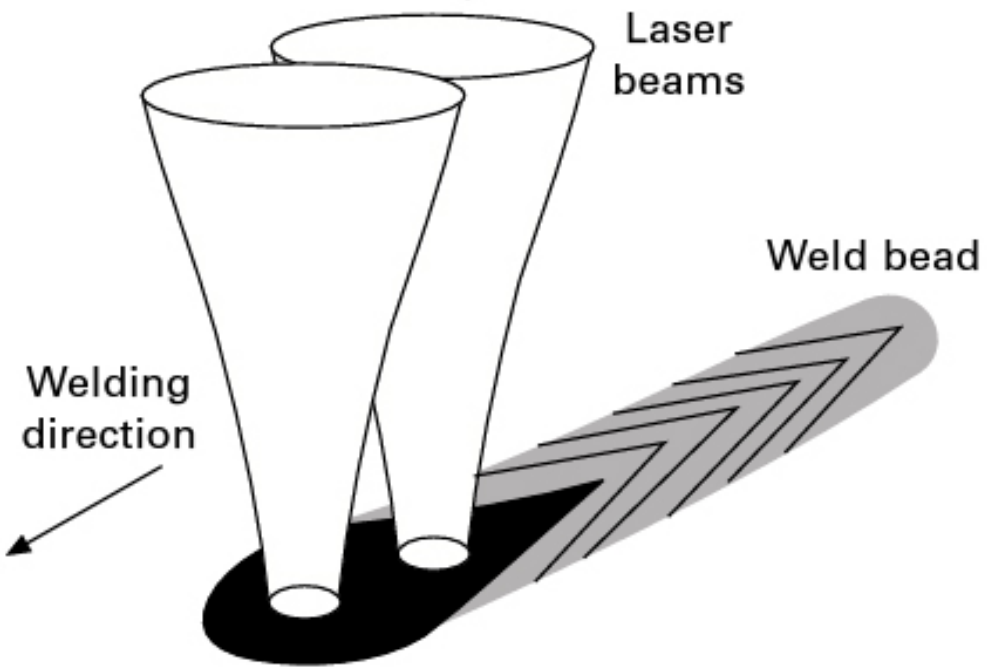

Figure 4. Configuration of twin-beam irradiation [5].

Twin-beam technique can be realized in two ways. The first one is to use two laser sources (figure 5), so the parameters can be set independently for each of the beams. Downside however lies in size and complexity of such set-up, as it requires very accurate optical alignment. The second way is adding an optic element into the set-up to split the beam (figure 6). This method easier to realize and also less costly. However, as the beam is origination from a single source, the phenomena related to combining two different laser sources can not be realized.

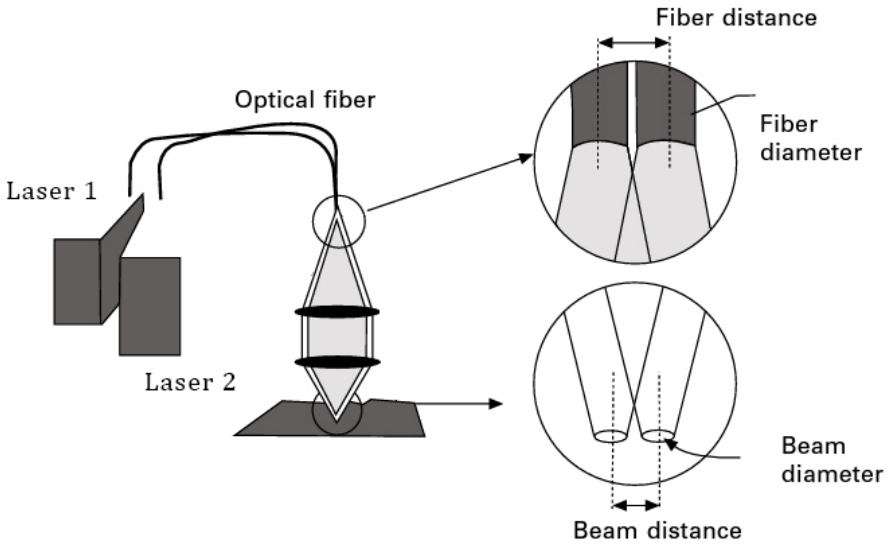

Figure 5. Twin-beam processing set-up produced by combining two lasers [5].

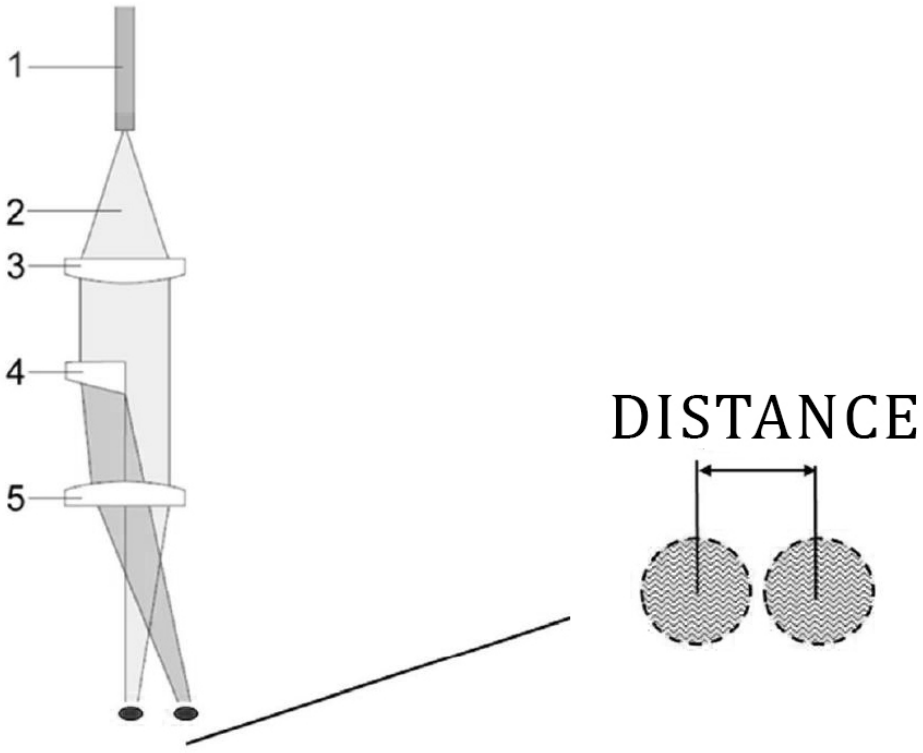

Figure 6. The principle and optical set-up of the twin-spot welding optic used in the welding trials. 1 - Laser light cable; 2 - Laser beam; 3. Collimator; 4 - Quartz glass wedge (twin-spot optic); 5 - Focusing lens. [6]

It was found [7] that combination of two beams can increase molten pool size and depth; the result of it shown on figure 7. Two materials with different properties have been presented.

On the (a) picture it shown that material having high thermal conductivity and high reflectivity has worse penetration than the one with low thermal conductivity (b). It was noted that absorption coefficient can be increased in some cases when two laser beams are used simultaneously.

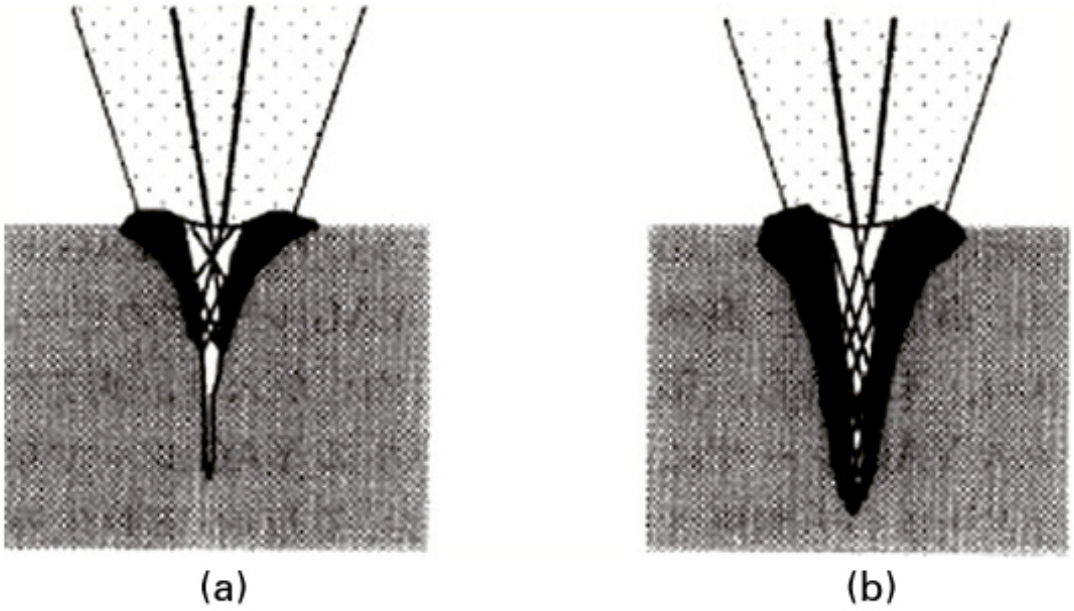

Figure 7. Effect of twin-beam laser irradiation on a highly reflective and highly thermal conductive material (a), and on low thermal conductive material (b) [7].

Other study [8] found correlation between beam distance for two Neodymium-doped Yttrium Aluminum Garnet (Nd:YAG) laser beams having different properties. It was found that increasing the distance between two beams leads to decreasing in penetration depth, and, that too small distance makes the process unstable. It was concluded that settings for the set-up have to be chosen carefully according to material parameters.

One reason for the application of dual-beam approach is to improve tolerance to air gap between two parts that need to be welded. The experiment, that is described in [9] featured wire-based twin-beam technique for achieving better results in laser welding with an air gap up to 1.6 mm. Longer distances were tested as well, but were resulting in not enough heat input because most of the energy was being transferred into the wire.

Using dual beam technique is also a viable approach to achieve better results in surface cladding. application of two beams versus one produces wider weld seam without losing any important characteristics. Similar results can be obtained with increasing the spot size in single beam set-up, however penetration depth was reduced. Two beams from one source or two different lasers provide wider irradiation zone compared with traditional single beam set-up (figure 8).

Figure 8. Illustration of weld shape for (a) single-beam and (b) twin-beam regimes.

2.2 Multi-pass laser welding with filler wire

Nowadays many applications for multi-pass laser welding technology exist, it is being extensively applied in pipeline production, shipbuilding, airplane construction and space engineering. The reason of it that in these fields welding sections with great thickness is required and it has to be done with minimal distortions. Initial cost of laser welding technology is higher than that of arc processes, however utilizing it reduces overall production costs and produces higher quality in shorter throughput time. Most important benefits are narrow weld seam, small heat affected zone, high joining efficiency and deep penetration. Laser beam welding may also be used in combination with arc welding processes. Adding a filler material and a second energy source increases the flexibility to the process by increasing gap tolerance and processing speed due to the fact that filler metal fills the space between parts and additional power source gives possibility to increase heat input that is lead to bigger productivity .

This technology can be applied even for welding sections with thickness up to 150 mm [10]. The illustration of the process (figure 9) shows a schematic drawing of the work area for the multi-pass technology. This process commonly requires careful groove preparation. The quality and form of the groove have significant influence on the process itself. There is a correlation between a groove angle and the amount of additional wire, less filler is required when groove angle is smaller. As was mentioned before, laser welding process gives very deep penetration so the decreasing in angle value will not become a problem for the reason that laser does not need go deep in the groove Based on gathered information it can be concluded that the best economic efficiency for multi-pass technique are achieved when the groove as tiny as possible.

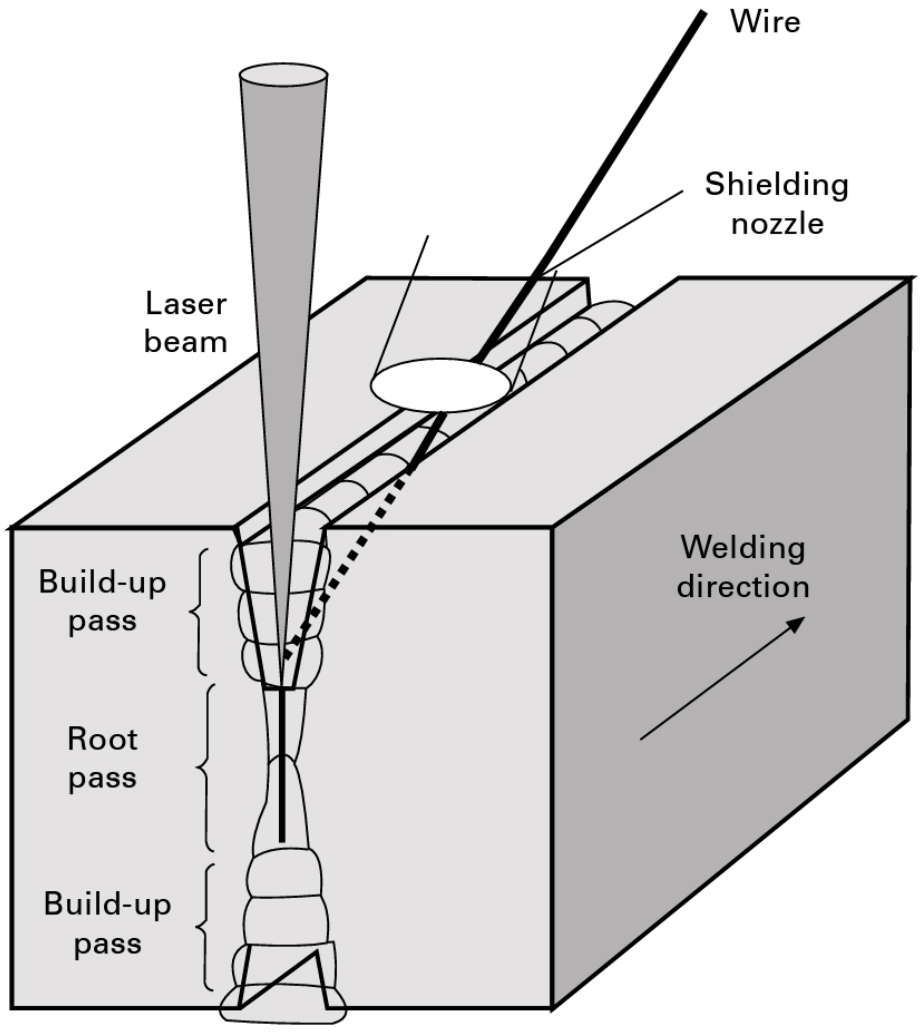

Figure 9. Schematic diagram of multi-pass laser welding with filler wire from both sides [11].

Root pass can be prepared with additional metal, but commonly it is not required. Following passes are always done with a filler wire. One of the main requirements to experimental set-up is the ability to achieve necessary power density nearby groove bottom position. Reason being that metal needs to be melted there despite the far point location from the laser welding head. It is achieved by using a high brightness beam with small spot size and a focusing lens with long focal length.

Welding set-up in case of multi-pass technique is illustrated on figure 10. It includes such base equipment as laser, optical configuration (lenses, mirrors, et cetera), positioning tool or robot hand, nozzle for shielding gas and the wire feed system. Seam tracking and monitoring/ registration systems also can be added.

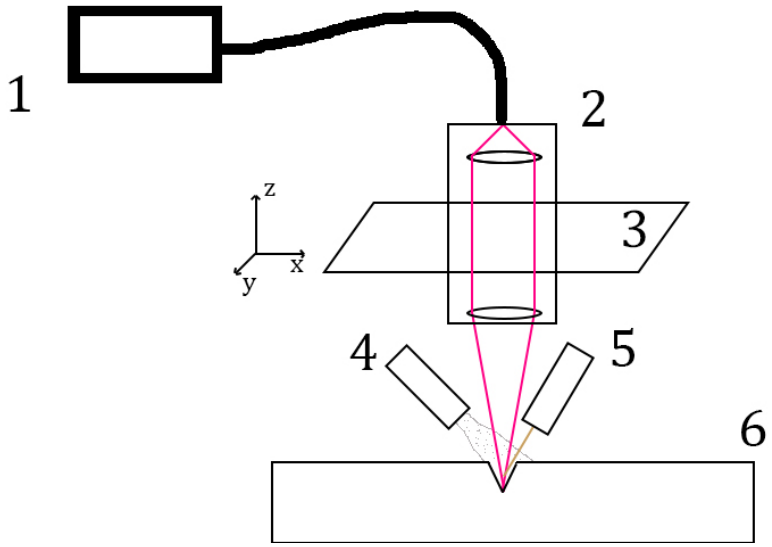

Figure 10. Illustration of common set-up for multi-pass welding. 1 – Laser; 2 – Optical configuration; 3 –Positioning tool; 4 – Shielding gas nozzle; 5 – Wire feed system; 6 – Workpiece.

As was mentioned before, multi-pass technique with additional wire is being commonly applied for ultra-thick sections, which are required long-time welding. That is the reason why one of the most important parameter is a long-time stability of the process that is has influence on the quality of the weld seam. For example, thermal focus shift can be a reason of changes in the focal point location. It has often happened in powerful laser systems when optical system is heated during long time exposure to multi-kilowatt beam.

2.3 Hybrid laser-arc welding

Currently, companies use those welding methods that are possible with accessible equipment. It is necessary to understand that the laser welding equipment that is nowadays provide the production process cannot be simply forgotten and replaced by another one, even in case when, for example, hybrid laser-arc welding (HLAW) can be more efficient. Manufacturing firstly must use the resource of the equipment that they already have. In addition, the change of manufacturing technology and the development of a new one require wasting a lot of time and money. For this reason, the researcher may notice that there are sufficiently effective technologies that are not currently used because of the high cost, but can be used in the future when their cost will decreases.

Modern welding manufacturing requires higher production rates, higher processing speed and shorter work cycles. However, it is also necessary to improve quality, or at least maintain it. Such situation creates the demand for novel welding techniques providing new features and better characteristics. Out of several known fusion welding processes (gas welding, arc welding and beam welding (figure 11) some of them can be combined to realize benefits from each technology. One possible combination is hybrid laser-arc welding, where beam and arc are interacting in a same melt pool.

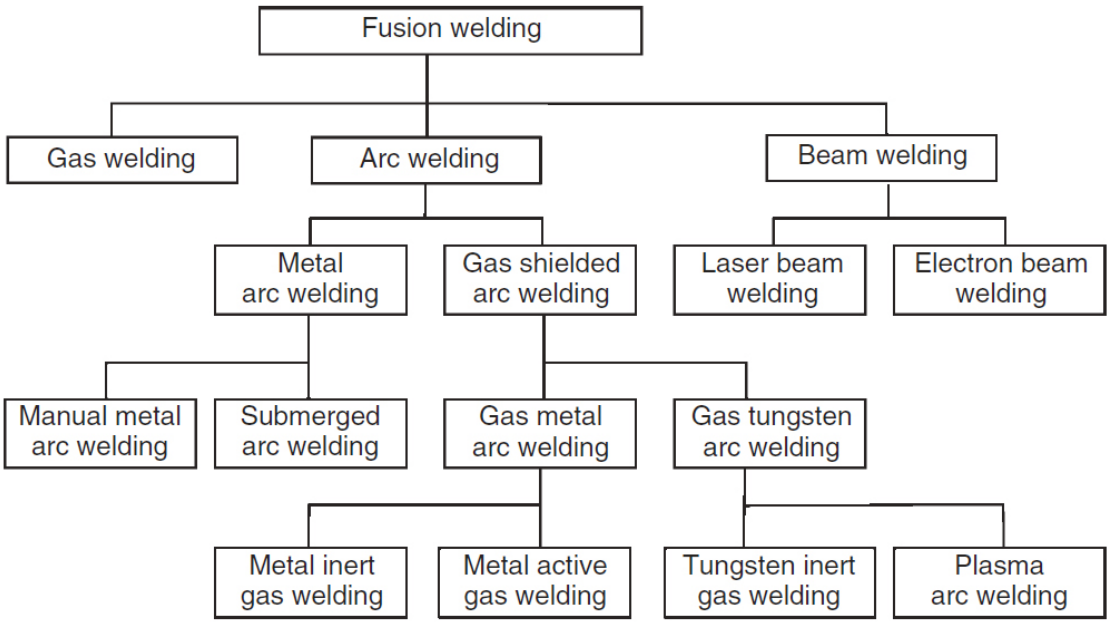

Figure 11. Schematic presentation of the most common fusion welding methods [12].

HLAW combines the energy of the electric arc and the laser beam, thereby providing many advantages against traditional methods. Hybrid process has higher deposition rate, better process efficiency, and higher stability of the process. It was observed that stability of an arc process improves when it works with the laser beam at the same time in same melt pool [13]. Hybrid laser-TIG (Tungsten Inert Gas) arc and laser-MIG (Metal Inert Gas) are shown on figure 12. The laser beam works in a keyhole mode and gives very deep penetration. In addition, arc process helps to increase air gap tolerance so it can be used even with a bad joint preparation. Additional filler wire can improve chemical composition of the weld pool, which is a reason of better seam quality.

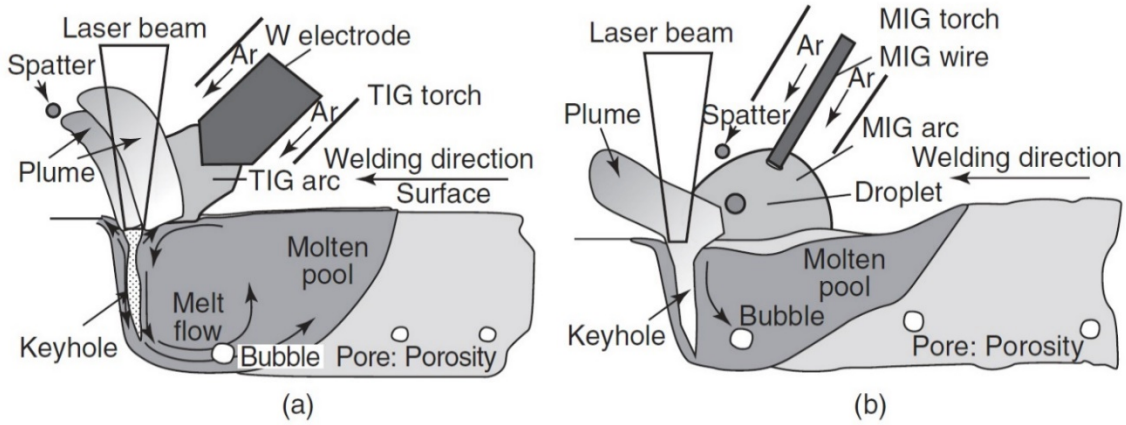

Figure 12. Schematic representation of hybrid laser–TIG (a) and laser–MIG welding [14].

The process can be applicable as for thin plates as for heavy sections. Many of required parameters such as heat input, penetration depth and filler wire have a major influence on the proper choice of the laser and the arc process.

3 DED

3.1 Introduction of DED

DED (Directed Energy Deposition) is an AM process or so called 3D printing. This process is commonly used for small or middle size parts with unusual or complex form. All of the AM processes, including DED, are mostly applicable for tasks where any other types of manufacturing methods can not be used due to limitations, for example when it requires light weight [15].

DED with wire is a process that uses laser radiation to create parts with layer-by-layer melting of filler wire. Laser beam heats focused area on the surface of the part, melts additional material and then move creating three-dimensional object which solidifying by cooling down (figure 13). This process requires laser source, wire feeder and shielding gas for protecting melting pool from oxidation and in some cases from plasma generation (figure 14).

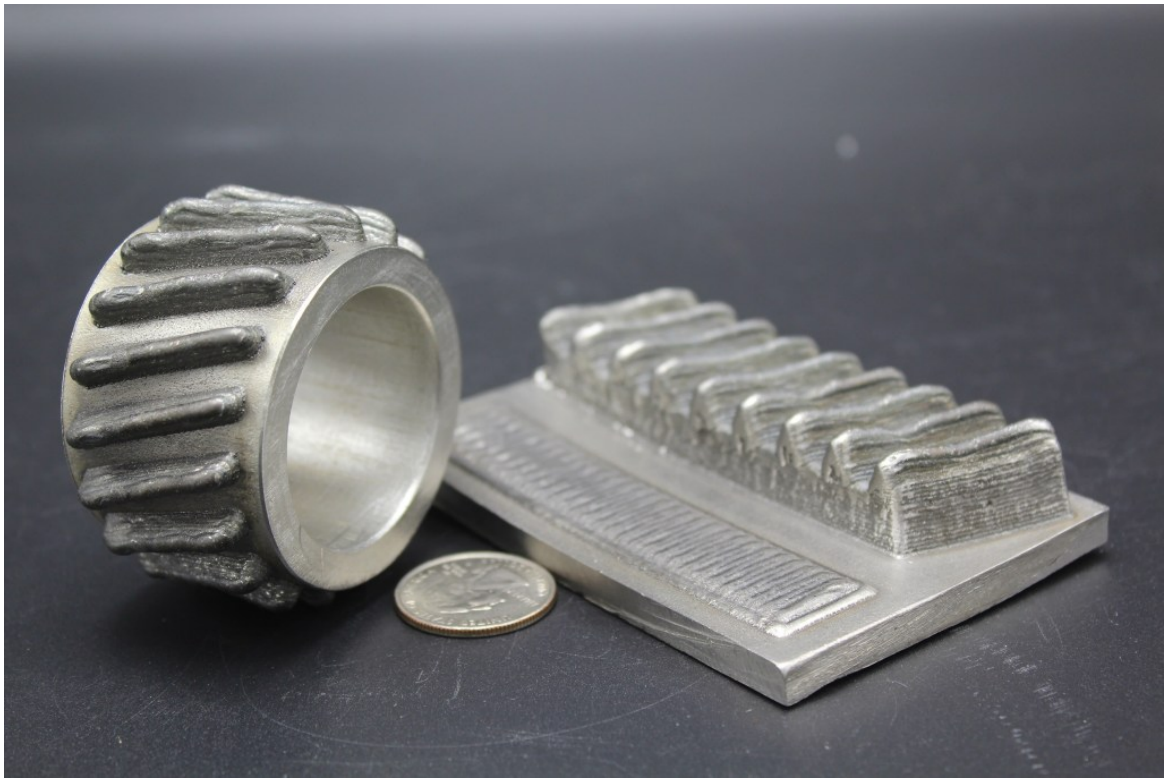

Figure 13. The example of AM product [16].

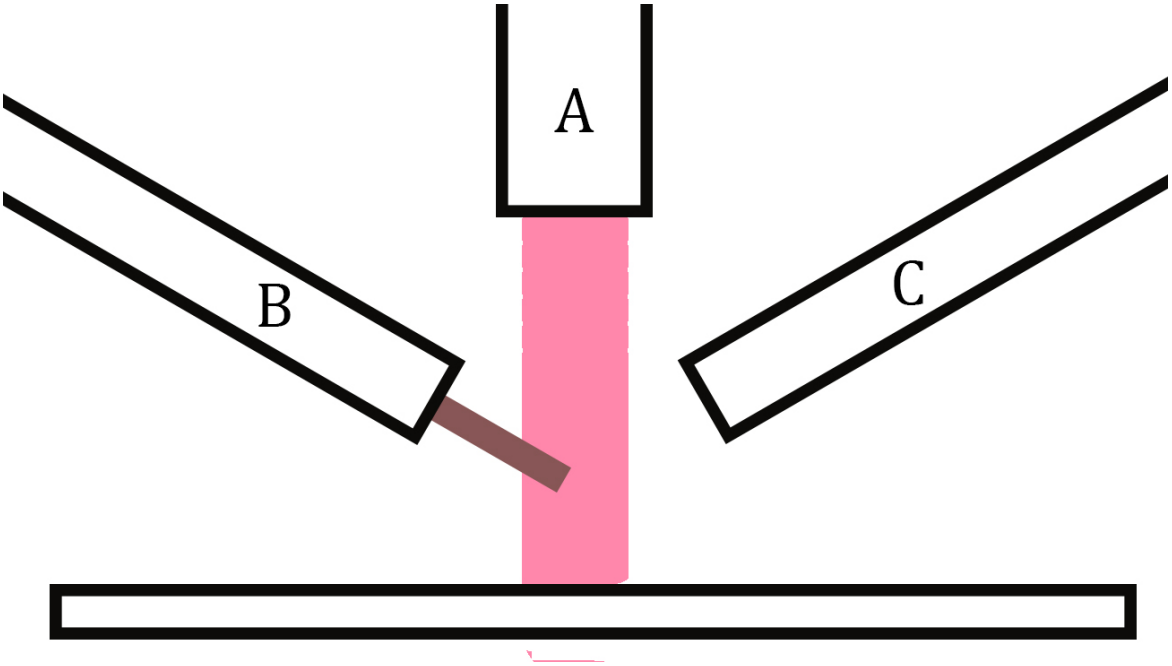

Figure 14. Illustration of a common setup for wire based DED process. Where A is a laser, B is a wire feeder, C is a shielding gas nozzle.

DED as a manufacturing method provides numerous benefits. It does not require some of pre-manufacturing steps such as production of new press-forms, calibrating and setting up of equipment in pre-and post processing stages of production, or, complex logistics arising from planning of whole production chain considering different stages. DED process requires only creating of design and producing it from start to finish in single step, with only possible post-processing action being surface polishing. DED is very similar to Powder Bed Fusion (PBF) process with difference that DED uses to melt material that is deposited, not pre-laid. Nowadays one of the main areas of application of DED is high quality repair of industrial machine components. Depending on requirements, DED can be preformed with powder or wire feed. There is one main advantage of using filler wire when comparing to powder. Powder has higher risk of porosity occurrence inside of the structure, and avoiding this is strictly important in most of applications. With wire, DED is capable to produce a pore free state, however accuracy is less than possible with powder use. Almost all of the wire material that is brought to the process is deposited, meaning that volume of filler wire fed into melt pool, except a small amount of spatter on the surface of work zone, is used

Additive manufacturing starts several decades ago when rapid prototyping (its “parent” technology) was used for manufacturing non-structural samples. Nowadays, additive

manufacturing uses in aerospace, car production and in many other fields (table 1). The main feature of the technology is possibility to create complex shapes. DebRoy T. et al. " [17, p. 116] wrote that "metal AM is now finding acceptance for critical applications such as medical implants, aerospace, and in many other fields with a clearly demonstrated ability to produce complex shapes". For that reason, highly complicated units are become easier to product for manufactures.

Applications ← ↓ Alloys	Aluminum	Maraging steel	Stainless steel	Titanium	Cobalt chrome	Nickel super alloys	Precious metals
Aerospace	X		X	X	X	X	
Medical			X	X	X		X
Energy, oil and gas			X				
Automotive	X		X	X			
Marine			X	X		X	
Machinability and weldability	X		X	X		X	
Corrosion resistance			X	X	X	X	
High temperature			X	X		X	
Tools and molds		X	X				
Consumer products	X		X				X

Table 1. Common additive manufacturing alloys and application [17].

Cladding, prototyping and welding are kind of basics for understanding additive manufacturing of alloys. Knowledge in these spheres is necessary but not enough to understanding all critical aspects of the AM process.

3.2 Rules and limitations

Wire based AM is using for generating bigger samples. But wire as the material in DED has several problems. Residual stress and distortion because of extreme heat input, poor part

accuracy caused by bad surface preparation. It also require proper control many of parameters such as welding speed, wire diameter, wire-feed speed and others. Nevertheless, the main problem in case of DED with wire for production huge parts is a residual stresses-induced deformation, which lead to the formation of cracks. In addition, strength, risk of porosity, hardness and other characteristics of the product is a question of proper process control. That is the reason why carefully parameter's setting and surface preparing are so important.

In case of wire-based system, it is very important to control position of wire because it effects condition of deposited metal and drop transfer characteristics. There are three positions: front, back and side feeding. It was found [18] that side and back speed feeding is finite for Nickel and Titanium alloys.

Wire speed is restricted by the power source. If it is high, metal will not 100% melted and only a part of it starts melting because of extremely big energy amount inside of melting zone. The meaning of the deposition rate can be found from counting input parameters of the wire diameter and feed rate. It is also was found [19] that output parameters of the operating zone are depended from the feed rate. Other main dependencies are shown in table 2. In comparison with powder bed technology, DED with wire has significant deposition rate due to large and defocused beam. In overall, there is not only one major condition to create a high quality structure; the process of DED itself is a complex solution with considering many of settings.

Table 2. Relations between DED parameters [19].

	Deposition area	Structure height	Structure width
Laser power ↑	X	↓	↑
Welding speed ↑	X	↑	↓
$\frac{\text{Wire feed rate}}{\text{Welding speed}}$ ↑	↑	↑	X

↑: increasing, ↓: decreasing, X: no effect

4 REGISTRATION TECHNIQUES AND MODELING

In welding and AM, researchers have a very important target. They need to find optimal parameters for any kind of material and application they are used for. It consist of mechanical and metallurgical properties and depends on necessary welding condition. Commonly, these studies concentrate on analysis of ready weld seam and on the molten pool shape through the welding process. For example, in the study [20] it was found that well-directed control in case of zinc-coated steels welding helps to prevent chaotic character of the pool and make it more stable. Mostly, to clear understanding of the process characteristics, it requires long experiment series that is take a lot of time.

The experimental study is used to explore the condition of a surface and the molten pool. One of the common nondestructive approach to get the information form the weld seam is X-ray transmission observation [21]. It gives a quite good picture of the weld seam and researcher can see not only molten pool shape but also a different defect formation such as porosity and bubbles (figure 15). One of the main benefit of the technique is that it is not necessary to destroy a sample. Unfortunately, the equipment costs a lot and it is heavy. In addition, this approach commonly does not provide live-time picture of the process.

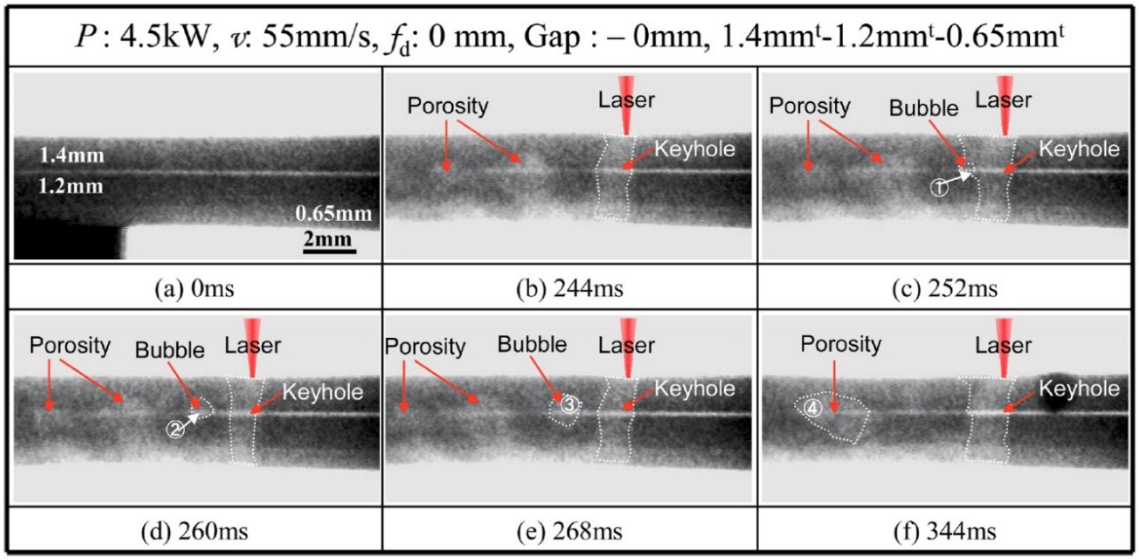

Figure 15. X-ray transmission observation results of keyhole behavior, bubbles, and porosity formation during laser lap welding of three sheets without gaps [22].

In case of laser welding, modeling and analyzing procedures commonly aim to a molten pool condition and a keyhole formation. As it known on of the main laser welding feature is a very deep penetration. Unfortunately, this vapor channel is very unstable and that is a reason why spatters [23] and pores [24] are formed. The keyhole shape is quite dynamic through the process and it depends on wire, base metal and process characteristics. One of the reasons of this instability is changes in light absorption that is depend mostly on temperature of the molten pool [25]. It is also influenced by multiple reflections inside a keyhole [26]. This instability leads to pores formation. The defect has bad influence on the residual stress. Spatter formation is another one problem; it leads to molten metal loses and requires additional surface cleaning after the process.

There are different ways to prevent this kind of instability. Stabilization gas can be added to keep keyhole as wide as possible; it helps to save channel from collapse [27]. Vapors can leave keyhole through another “window” in case of full penetration method; it helps to increase stability of the process [28]. Small atmosphere pressure can reduce the amount of spatters [29]. These methods help to stabilize the system. Understanding of them is necessary to successful choice of applicable approach.

Unfortunately, measurement of keyhole properties is a big problem for the reason that an area that is near by the molten pool has extra high temperature and very big pressure. However, researchers also have methods to control it indirectly, for example optical process emissions [30].

One of the most popular direct technique is a registration of molten pool form with ultra-high speed cameras. It works with a photo filter, which is work with a narrow area of wavelength. The reason of it is to not damage camera and to achieve higher picture quality without noise. In some cases, real-time X-ray imaging can be used to observe a processes inside a keyhole.

Laser-based manufacture processes need in proper temperature control of substrate. It is a tricky task because laser beam change the location very fast and the distribution of the energy field changes many times through the process. Nowadays, the most favorite way to registration of the temperature is using thermocouples. Unfortunately, they are measuring

only narrow area where they are located and do not provide complex 3D model of the temperature gradient.

One of the way to solve this problem is to create virtual 3D model of temperature distribution and check if it is correct or not by comparing it with experimental data. The example of such type of model is illustrated on figure 16. The laser beam hits the sample's surface and heat spreads inside of metal creating different heat zones, which are similar to common laser welding process. The illustration on figure 17 shows that sample has four different areas: weld interface (WI), heat affected zone, untouched parent metal (PM) zone and liquid phase region of welded metal (WM).

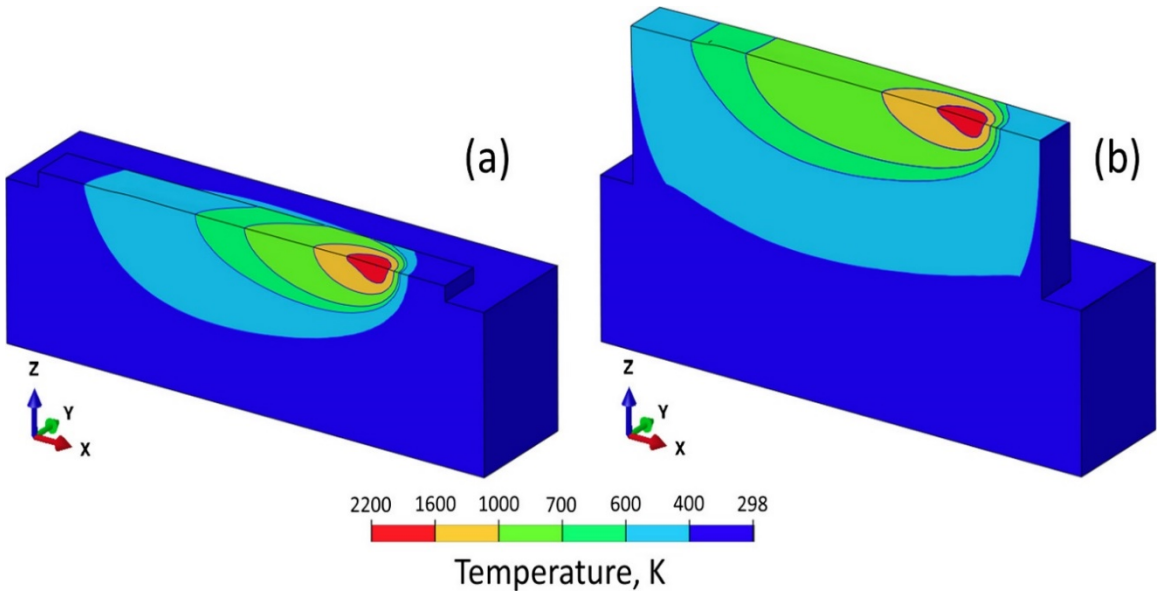

Figure 16. Virtual 3D model of temperature gradient in AM for first (a) and tenth (b) layer [17].

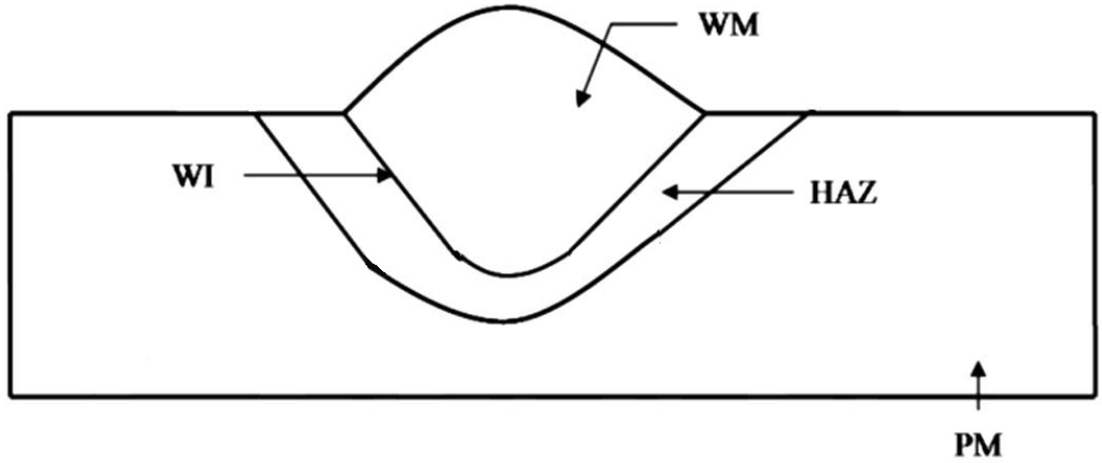

Figure 17. The illustration of heat zones where PM is parent material, HAZ is heat affected zone, WI is weld interface and WM is welded metal.

Heat affected zone is located near to the welded metal area. In this space, the material receives the amount of energy that is not enough to start melting process; however, it is a quite large temperature that is lead to microstructural changes inside of the solid area which is critical in case of achieving high quality product. The WI is a melted or partially melted base material that is liquid throughout the heating process, but it becomes hard until it mixes with welded metal zone; a small border that divides two nearest zones from each other. The liquid phase are contains of the additional wire and the base material which is melted. It is a first stage in energy transfer rout. This region requires researcher to priority focus on it because of the most important processes take place here such as evaporation, oxidation and solidification. Possible defects will be described in the next chapter. The last, PM zone does not get any significant impact from the high temperature. Therefore, PM is like a shell for HAZ, so it can figure out some problems related to residual stress, which is an outcome of structural material changes inside HAZ.

Nowadays, the most modern way to observe the condition of the processes which are cannot be measured is modeling. It gives many advantages benefits but also has some disadvantages (table 3). There are many of different numerical techniques to simulate processes inside the keyhole; unfortunately calculations takes a lot of time [31]. Opposite, analytical approach requires spending less time but it is necessary to simplify it. For example keyhole oscillations can be described by analytical approach; the study [32] explored the relations between vapor flows and radius width in the different depth of the keyhole.

Table 3. Advantages and disadvantages of modeling in laser welding.

Advantages	Disadvantages
Complex map of the process	Require to take into account many of parameters
Real experiment is not necessary	Hard to realize
Save a lot of time when ready	Waste a lot of time from beginning to ready-to-use
Save a lot of money when ready	Costs a lot while in production phase
Decrease in amount of pre-manufacturing steps	Require powerful computer
Gives results before manufacturing start	

5 DETECTORS

In manufacture, it is necessary to measure as much parameters and aspects of the process as possible. More popular detection methods to achieve the best results in additive manufacturing are temperature and geometry control. There are several ways to do it.

5.1 Pyrometer

Pyrometer (figure 18) is a tool that detects intensive emission and transform it to electrical signal according with the settings that compare it with a temperature map. It is based on camera or photodiode. Like any tool, it also has some benefits and limitations. It can be placed strictly close to the working area near by laser and it will not influence on the process. The problem is a narrow application. Pyrometer can collect data only from the surface and does not provide complex solution to monitoring whole sample. It is often used like a part of complex set up that is help to measure temperature changes. However, it is more applicable to already explored metals because in case of completely new sample it requires to correct setting of a tool to proper transform collected data about emission intensity into the temperature meaning. Gas evaporation can add mistakes in measurement with pyrometer.

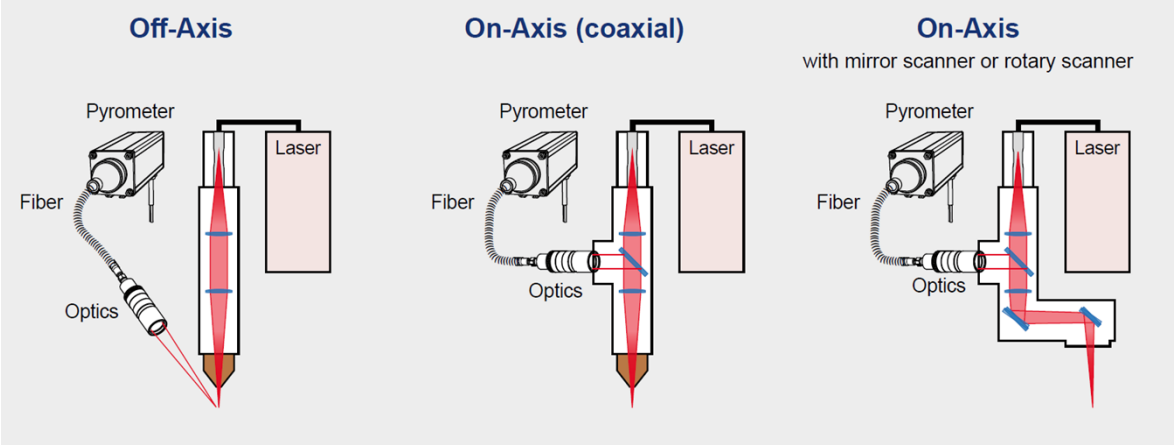

Figure 18. Different configurations of laser-pyrometer setup [33].

5.2 Thermocouples

Thermocouples also very often used by researchers because they are much cheaper than pyrometers. The main problem of this solution is that it is contact method, which provides information only about temperature first deposited layer and does not give information about

upper layers (figure 19). It mostly uses in research tasks for small experiments and almost never uses in real production for reason of that kind of limitation.

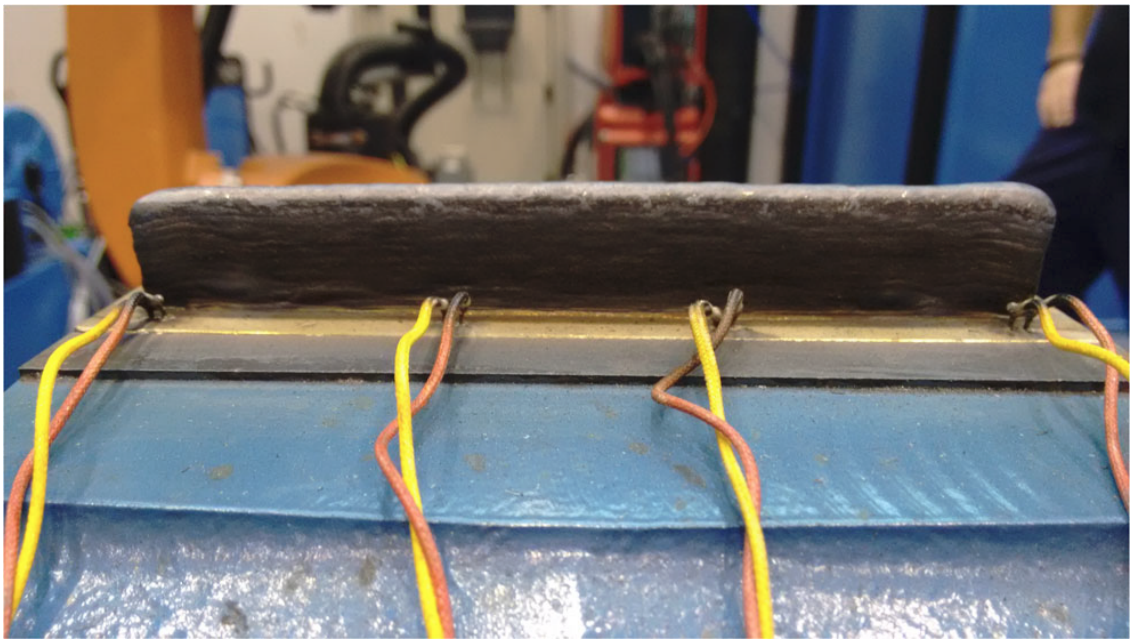

Figure 19. Thermocouple localization close to the first bead deposited layer [34].

5.3 High-speed camera

For real production and for laboratory there is one very important aspect that is ability to reproduction of previously achieved results. It is a big problem in case of DED because work piece geometry changes every time through the heat and cool cycles and melting pool also. Nowadays, the condition of the working area is mostly registered by super speed cameras, which are have ability to make impressive numbers of shots per second. One of the requirements to make a setup with this control technique is modern computers that can operate with collected data and show it in real time. Unfortunately, this approach gives information only about surface condition.

5.4 Spectroscopic monitoring

In the process of laser-based welding or AM, details are often overheating, it leads to the formation of porosity, cracks, insufficient penetration and other defects. This method is used when requirements for product quality are very high. Accordingly, the study of process control capabilities is an urgent task for improving the quality of results. The example of spectroscopic monitoring [35] shows results for chromium and nickel evaporation. Results

are shown on figure 20. This technique gives information about emission spectrum of alloys, which are evaporate from the surface of the molten pool.

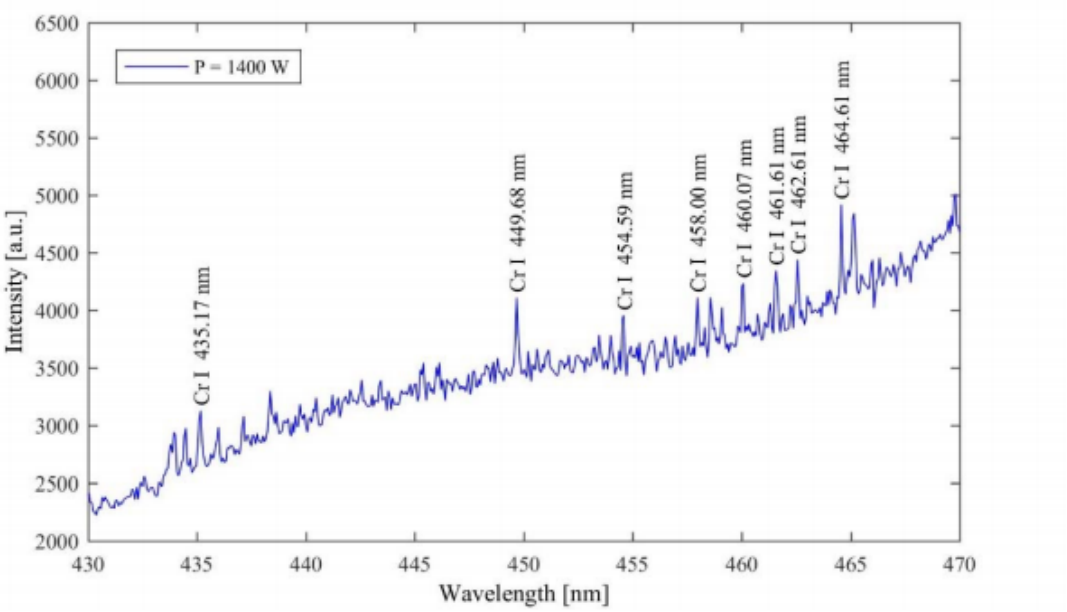

Figure 20. Emission spectrum with a wavelength range from 430 to 470 nm with a power of 1400 kW [35].

There are also other techniques to control welding and AM parameters. Mostly the production needs to apply several control units or their combination to achieve proper results. It also requires powerful analysis tools and techniques to transform collected information into usable for researcher form. One of the newest technique that gives better results and solves a problem with measuring rapidly changing sample's conditions is closed-loop feedback system. This system adapts to the changing inside a process and makes accurate changing in process parameters to prevent any mistakes and achieve the best result. However, such kind of system very difficult and not explored enough. That is the reason why nowadays they are not popular enough.

6 DEFECTS

Laser welding and AM processes are characterized by many advantages and can work in different environments (vacuum, air or shielding gas). Unfortunately, there are limitations that lead to defect formation, which happens due to incorrect choice of parameters. All manufacturing is trying to achieve high quality of product because it gives competitive advantage on the market. That is a reason why proper measurements, calculations and preventive procedures are important.

One of the defects is distortion or deformation. Different parts of the base material are heated and cooled many times through the process, some of the elements are evaporated changing metallurgical properties, which leads to cracks, residual stresses and distortion. It is more probable to happen when heat input is significant and melting pool is wide. Thin plates and especially materials that have high temperature expansion coefficient (for example, aluminum alloys) belong to such group of risk. In case of laser welding against other welding processes, bead width is commonly smaller, so it gives lower risk of distortion.

Another issue is evaporation loss of alloying elements. Through vaporization process, some particles of alloying elements leave the sample. It leads to increasing possibility of structural changes in the output composition [36] such as mechanical properties and corrosion resistance. One of the way to measure this meaning is spectrometry, a non-destructive observation method that has no influence on the process itself.

Porosity is also a common defect, and even replacing powder with wire does not guarantee samples being fully free of porosity. Shielding gas is often used to protect melting pool from porosity, however it also can be a reason porosity occurrence, although it is not very common. There is also a keyhole pore formation (figure 21a) when depositing in keyhole mode. In such arrangement, the size of pores depends on dimensions of the keyhole.

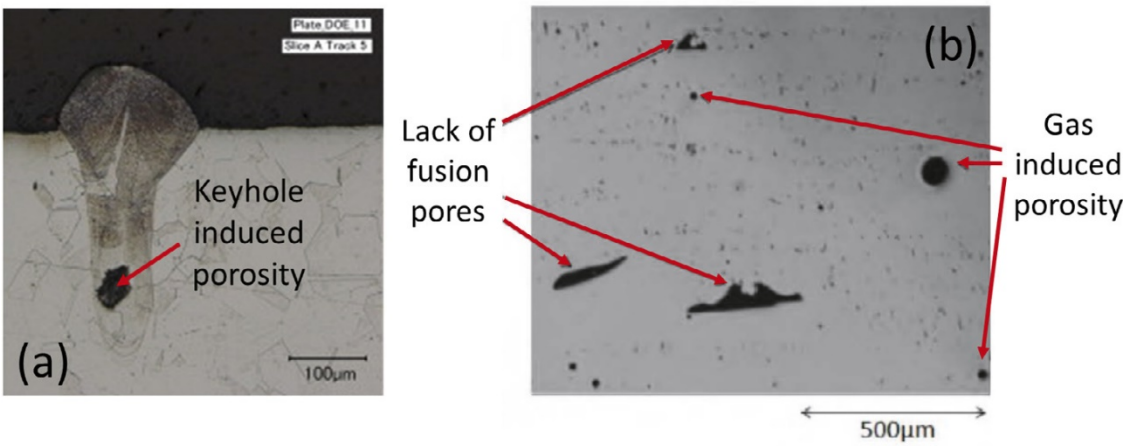

Figure 21. Pore formation by keyhole mode (a); lack of fusion and gas induced pores (b) [22].

Lastly, the lack of fusion defects, which have same causes of occurrence as porosity. Alternatively, the cause may be insufficient penetration of molten pool from higher layer to base metal or to the previous layer (figure 21b). Many other defects, reasons of their formation and prevention techniques of them are summarised in tables 4-6. Defects can be categorized in three groups: geometrical, internal and property related.

Table 4. Geometrical defects [37].

Name	Illustration	Causes	Remedies for prevention
Deformation (strain) (distortion)		Great thermal effect; Incomplete jigging and restraint condition	High speed, deep penetration welding; Utilization of rigid jig
Bad appearance (dirty surface) (rough surface)		Improper welding conditions	Low power density welding; Removal (blow-away) of evaporated particles
Drop-through (burn-through)	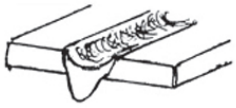	Thin sheet Wide bead width due to excessive energy	Optimization of welding conditions (lower heat)

Table 4 continues. Geometrical defects [37].

Name	Illustration	Causes	Remedies for prevention
Undercut		Slow welding speed and high heat input Properties of weld fusion zone (viscosity)	Proper welding conditions (gas, etc.)
Underfill	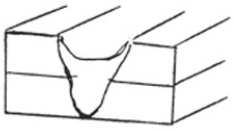	Spattering due to excessively power density and small melt zone	Avoidance of low energy and focused conditions; Optimization of pulsed laser welding

Table 5. Internal defects [37].

Name	Illustration	Causes	Remedies for prevention
Crack (hot crack) (solidification crack) (liquation crack) (crater crack) (bead crack) (cold crack)		Low melting point products and segregation; High stress/strain (rapid strain rate)	Proper selection of alloying compositions in weld metal and base metal; Optimization of pulsed laser welding; Avoidance of high speed welding; Prevention of rapidly augmented strain-rate
Porosity (blowhole) (pore) (pit)		The absorption of nitrogen, oxygen and hydrogen in the molten weld pool	Elimination of hydrogen and oxygen sources; Formation of stable keyhole; Proper selection of shielding gas and flow rate

Table 5 continues. Internal defects [37].

Name	Illustration	Causes	Remedies for prevention
Crack (hot crack) (solidification crack) (liquation crack) (crater crack) (bead crack) (cold crack)		Low melting point products and segregation; High stress/strain (rapid strain rate)	Proper selection of alloying compositions in weld metal and base metal; Optimization of pulsed laser welding; Avoidance of high speed welding; Prevention of rapidly augmented strain-rate
Porosity (blowhole) (pore) (pit)		The absorption of nitrogen, oxygen and hydrogen in the molten weld pool	Elimination of hydrogen and oxygen sources; Formation of stable keyhole; Proper selection of shielding gas and flow rate
Incomplete penetration Lack of fusion		High reflectivity and effect of plasma	Proper conditions for deep penetration; Prevention of misalignment
Inclusion (oxides, etc.)		Interaction of foreign materials	Surface polishing; Proper shielding conditions
Evaporation loss of alloying elements	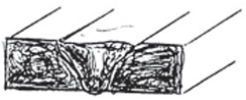	Volatile elements and low temperature of melt	High-speed, deep-penetration welding; Pulsed deep-penetration welding
Macrosegregation		Incomplete mixing of dissimilar materials	Mixing due to beam oscillation or pulsation;

Table 5 continues. Internal defects [37].

Name	Illustration	Causes	Remedies for prevention
Microsegregation		Elements of low distribution coefficients	Welding at high speed and low heat-input; Solution heat treatment after welding

Table 6. Property defects [37].

Name	Illustration	Causes	Remedies for prevention
Crack (hot crack) (solidification crack) (liquation crack) (crater crack) (bead crack) (cold crack)		Low melting point products and segregation; High stress/strain (rapid strain rate)	Proper selection of alloying compositions in weld metal and base metal; Optimization of pulsed laser welding; Avoidance of high speed welding; Prevention of rapidly augmented strain-rate
Porosity (blowhole) (pore) (pit)		The absorption of nitrogen, oxygen and hydrogen in the molten weld pool	Elimination of hydrogen and oxygen sources; Formation of stable keyhole; Proper selection of shielding gas and flow rate

7 WIRE VERSUS POWDER

The laser- AM and welding processes can be performed with an additive material in the form of wire and powder. The use of wire is not very common now and, according to Scopus data, was not investigated good enough. An analysis of articles uploaded to the Scopus scientific database was carried out. For keywords, titles and a brief description, a search was made and it was found that the number of articles on direct energy deposition with powder significantly exceeds the number of articles on wire (figure 22). But interest in wire feeding systems is growing, as this method is more cost efficient and metallurgical quality is better.

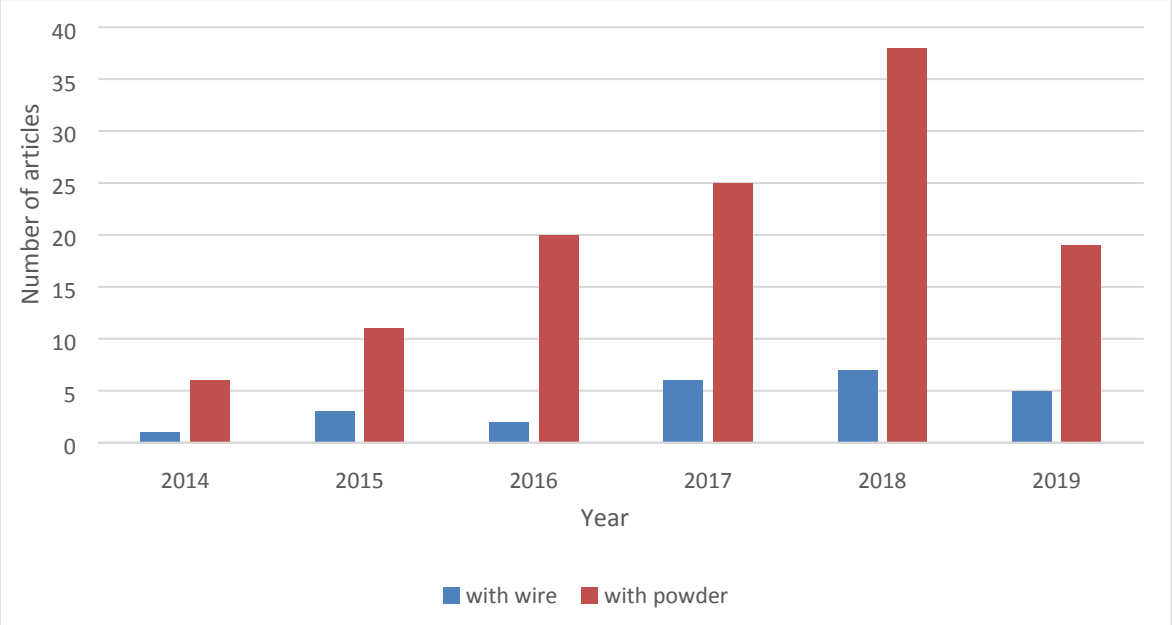

Figure 22. Analysis of the number of articles in Scopus in the field of directed energy deposition in the period from 2014 to 2019.

There are some reasons to use wire against powder. For example, the powder is difficult to apply in a vacuum environment due to the ionization of the gas. Also, there is much less oxygen in the wire, which reduces the risk of a defect such as porosity. Again, in the case of electron beam welding, the efficiency of wire use is 100%, and in most cases the powder has only 50%. However, in the case of powder, it is possible to reuse up to 9 times, which is environmentally friendly and economical [38]. No examples of recycling and reuse of wire were found in the literature.

The deposition rate of the wire can reach very large values, but at the same time, because of this, there is a risk of formation of rough surfaces that require careful post-processing. There is also a double wire feed system. Its feature is the simultaneous use of two wires at once, which can be of different sizes and compositions. To control the size of the parts produced using wires of different diameters. So, for small parts is chosen wire with a small diameter, and for large - the largest. The smallest part size that can be created is determined by the diameter of the wire.

The composition of the wires may vary depending on what mechanical properties are needed. According to The Grainger Catalog [39], which is a major supplier of wires, there are 380 variations of welding wires only from steel and nickel alloys. Wires are made from other materials, but they are not represented in the Grainger Catalog. Figure 23 shows the materials from which the wire can be made.

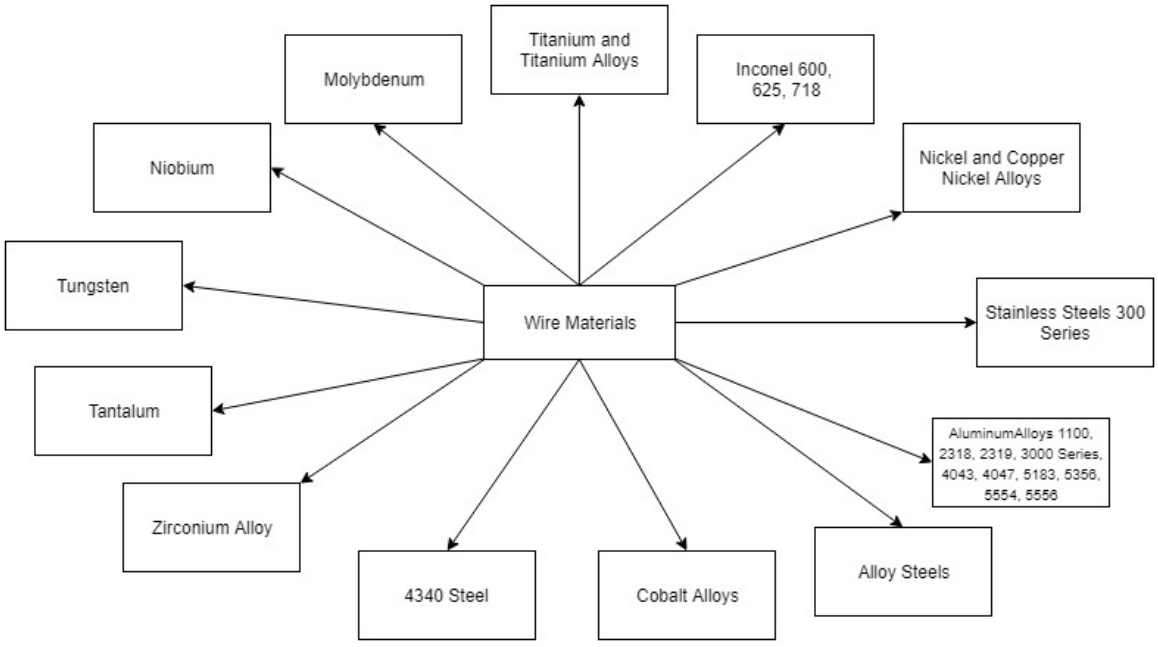

Figure 23. The materials used to make wires for direct energy deposition [39].

The cost of the wire is much higher than that of the powder. Data on the cost of the powder was taken on the website of the company Sciaky inc. [40]. Comparing prices, it can be seen that, for example, the cost of the Inconel 625 was a maximum of $65 per kilogram, while the powder cost $ 120, which is almost 2 times more expensive. This trend is visible with all

the above materials, except for Tantalum, the cost of which is about the same in both cases. The data is shown on figure 24 reflects prices in the USA market in 2015.

Material Feedstock	Titanium 6Al-4V	Tantalum	Inconel 625	Stainless Steel 316
Wire—0.035" Diameter (0.9 mm)	$58/lb.	$545.30/lb.	$26.73/lb.	$5.19/lb.
Wire—0.045" Diameter (1.1 mm)	$54/lb.	$545.30/lb.	$23.30/lb.	$4.63/lb.
Wire—0.062" Diameter (1.6 mm)	$50/lb.	$524.88/lb.	$22.17/lb.	$4.57/lb.
Wire—0.093" Diameter (2.4 mm)	$48/lb.	$502.30/lb.	$21.43/lb.	$4.81/lb.
Wire—0.125" Diameter (3.2 mm)	$45/lb.	$438.96/lb.	$21.02/lb.	$4.75/lb.
Wire—0.156" Diameter (4.0 mm)	$44/lb.	$438.96/lb.	N/A	$4.69/lb.
Powder—AM Grade	$120/lb.	$522/lb.	$48/lb.	$10/lb.

Figure 24. Market value of powders and wires for welding in 2015 in the USA [41].

8 RESEARCH METHODS

8.1 Set-up

The research work carried out in scope of this thesis included two different set-up configurations. The first one was used to determine the location of the beam reflected from the wire. The second one was performed for measuring the intensity of reflected beam. The schematic visualization of the first set-up is illustrated on figure 25. Live photos of the main set-up components are shown on figures 26 and 27.

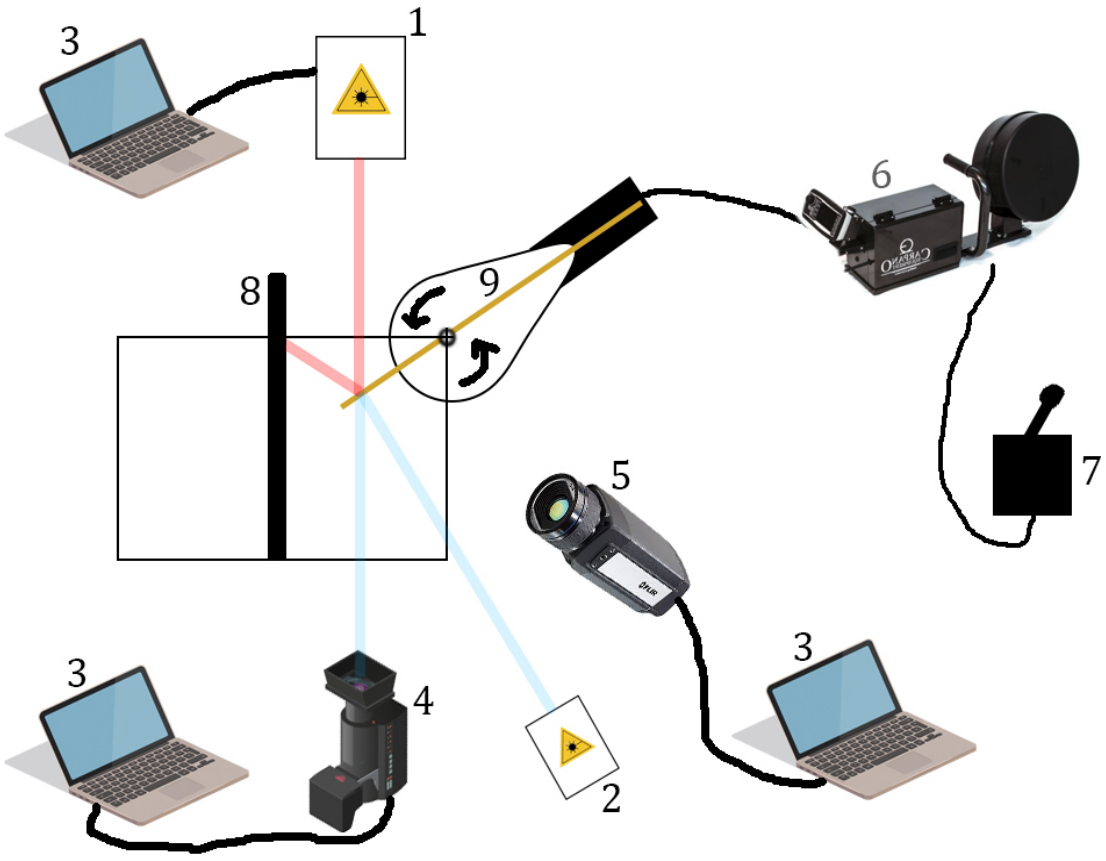

Figure 25. Schematic visualization of the set-up. 1 - laser processing head of ytterbium laser system “YLS-10000-S4”; 2 – Illumination laser “CAVILUX HF” 500 W, 808 nm; 3 – Laptop with software; 4 - High speed camera “Navitar Optronics cr3000×2”; 5 - Infra-red camera “FLIR A615”; 6 - Wire Feeder “Carpano Equipment VPR-4WD”; 7 – Start/stop switcher for wire feeder; 8 – 2 mm thick bBlack-painted plate (2 mm stainless steel 304); 9 – Feed nozzle with carbon-manganese steel wire “OK Autrod 12.64”.

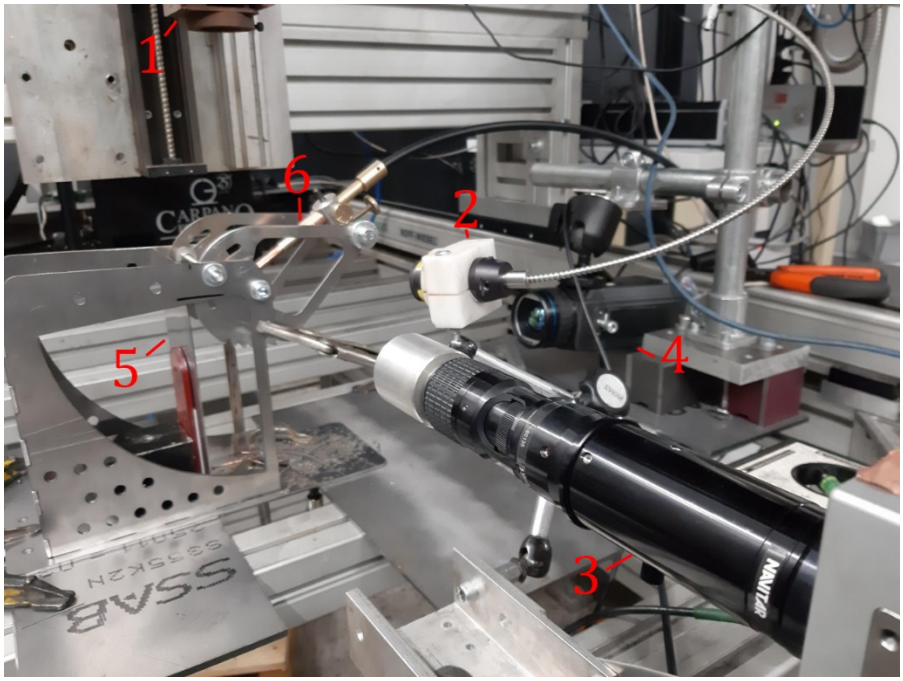

Figure 26. Real photo of the set-up. 1 - laser processing head of ytterbium laser system "YLS-10000-S4"; 2 – Illumination laser "CAVILUX HF" 500 W, 808 nm; 3 - High speed camera "Navitar Optronics cr3000×2"; 5 - Infra-red camera "FLIR A615"; 5 – 2 mm thick bBlack-painted plate (2 mm stainless steel 304); 9 – Feed nozzle with carbon-manganese steel wire "OK Autrod 12.64".

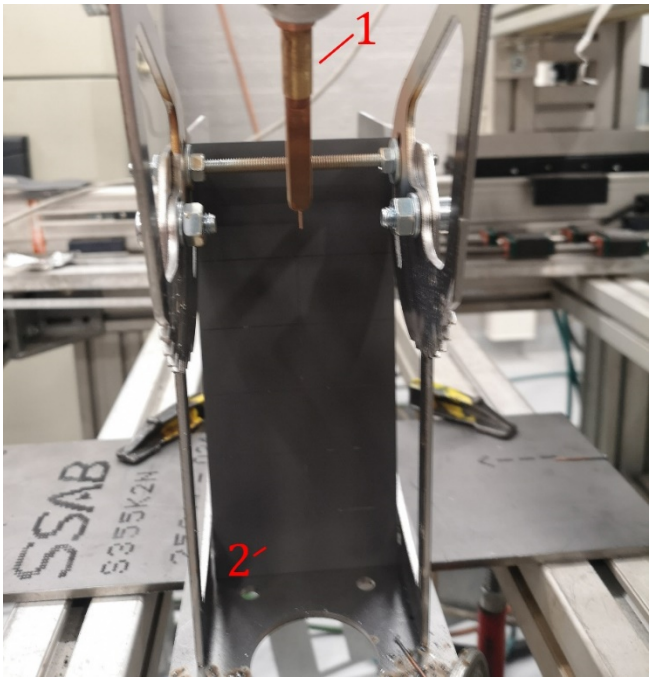

Figure 27. Real photo of the set-up. 1 – Feed nozzle with carbon-manganese steel wire "OK Autrod 12.64"; 2 – Black-painted plate 2 mm stainless steel 304.

High-speed camera was equipped with a light filter working at wavelength of the illumination laser. Infra-red camera was used to take a video of heated area of the black-painted plate. Process was being recorded with a high-speed camera to estimate when the process becomes unstable. The position of cameras was fixed throughout all measurements. Stainless steel sheet was colored by black paint for the reason of giving better absorption of the reflected laser beam. The scale with a step of 30 mm was drawn on the plate to better understanding of the reflected light area (Figure 28).

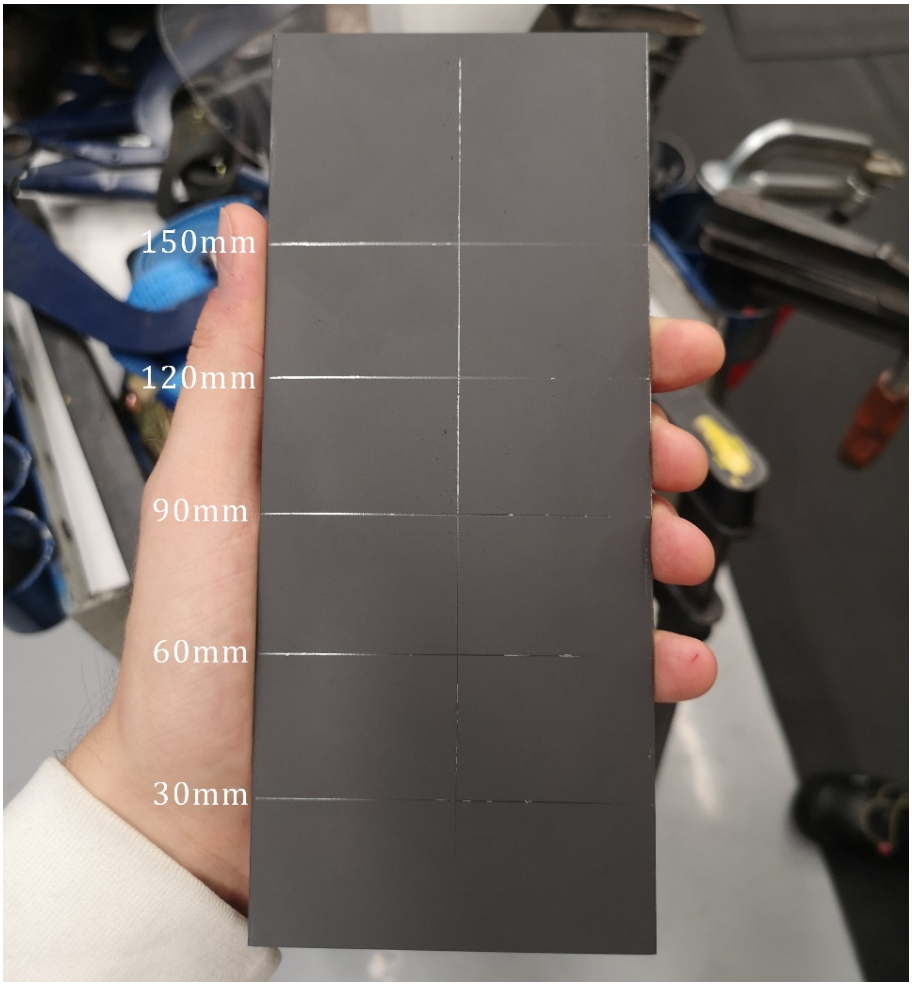

Figure 28. Photo of the Black-painted plate with a marked scale.

Copper-coated carbon-manganese steel (Mn/Si-alloyed) wire “OK Autrod 12.64” was used in the study. The chemical composition is shown in table 7. Ytterbium laser system “YLS-10000-S4” was used as a power source. The characteristics are shown in table 8.

Table 7. Chemical composition of the wire "OK Autrod 12.64" [41].

C, %	Mn, %	Si, %
0.074	1.68	0.95

Table 8. The characteristics of Ytterbium laser system "YLS-10000-S4" [42].

Characteristics	Meaning	Unit
Operation Mode	Continuous wave	
Polarization	Random	
Nominal Output Power	10	kW
Emission Wavelength	1070-1080	nm

8.2 Experimental part and analysis of it

8.2.1 First step

The study was done in the Laboratory of Laser Processing at LUT University. The experimental part and analysis are divided into several pats. The research questions were as follows:

- finding suitable parameters for obtaining stable melting of wire in conditions of available laboratory set-up;
- determining the location of the reflected laser beam using black-painted plate and infra-red camera;
- building a new set-up for measuring the intensity of reflected beam.

As it can be seen from the table 9, the first experiments were made using beam diameter of 0.4 mm (focal position 0 mm). When the Wire Feed Rate (WFR) achieved 3 m/min, the plate suffered damage (see figure 29) and it was decided to increase the beam diameter for reducing the power density. Smaller power density leads to lower maximum temperature in the reflected area and helps to prevent damaging of the plate. New plate was made from the same material. Series of experiments were continued with the diameter of the beam 0.76 mm (focal position +10 mm).

Figure 29. Photo of the damaged plate.

Table 9. Results and parameters from the first part of the experiment.

Wire angle, °	Power, kW	WFR, m/min	Beam diameter, mm	Focal position, mm	Comment
50	2	1	0.4	0	Big molten ball
		1.5			Spatters
		2			Big molten ball
		2.5			Better, but unstable
		3			The wire is melted in the middle, leaving the edges. The beam diameter should be increased. Plate was damaged.

8.2.2 Second step

In further experiments the aim was to investigate whether there are significant changes in the shape of reflected beam under different irradiation times. The reason being understanding whether the experiments can be done with the minimum possible irradiation time (to achieve more productivity of the experiment). Irradiation times of 2 seconds and 5 seconds were chosen. To verify the results, WFR was varied (1.0 m/min, 1.5 m/min, 2.0 m/min and 3 m/min), the parameters are presented in table 10.

Table 10. Parameters for the second step of the experiment.

Wire angle, °	**WFR, m/min**	**Time, s**	**Power, kW**	**Focal position, mm**	**Beam diameter, mm**
30	1	2	2	+10	0.76
		5			
	1.5	2			
		5			
	2.0	2			
		5			
	2.5	2			
		5			
	3.0	2			
		5			

Results are shown on figure 30. It can be seen from the temperature scale on the figure that peak meanings are different for different measurements. In scope of this study it was made for the reason that to show a matching of shapes is more important that the temperature meanings for the reason that main aim is to find a location of reflected beam. It can be concluded that there are no significant changes in the shapes. For this reason, study was continued with irradiation time of 2 seconds.

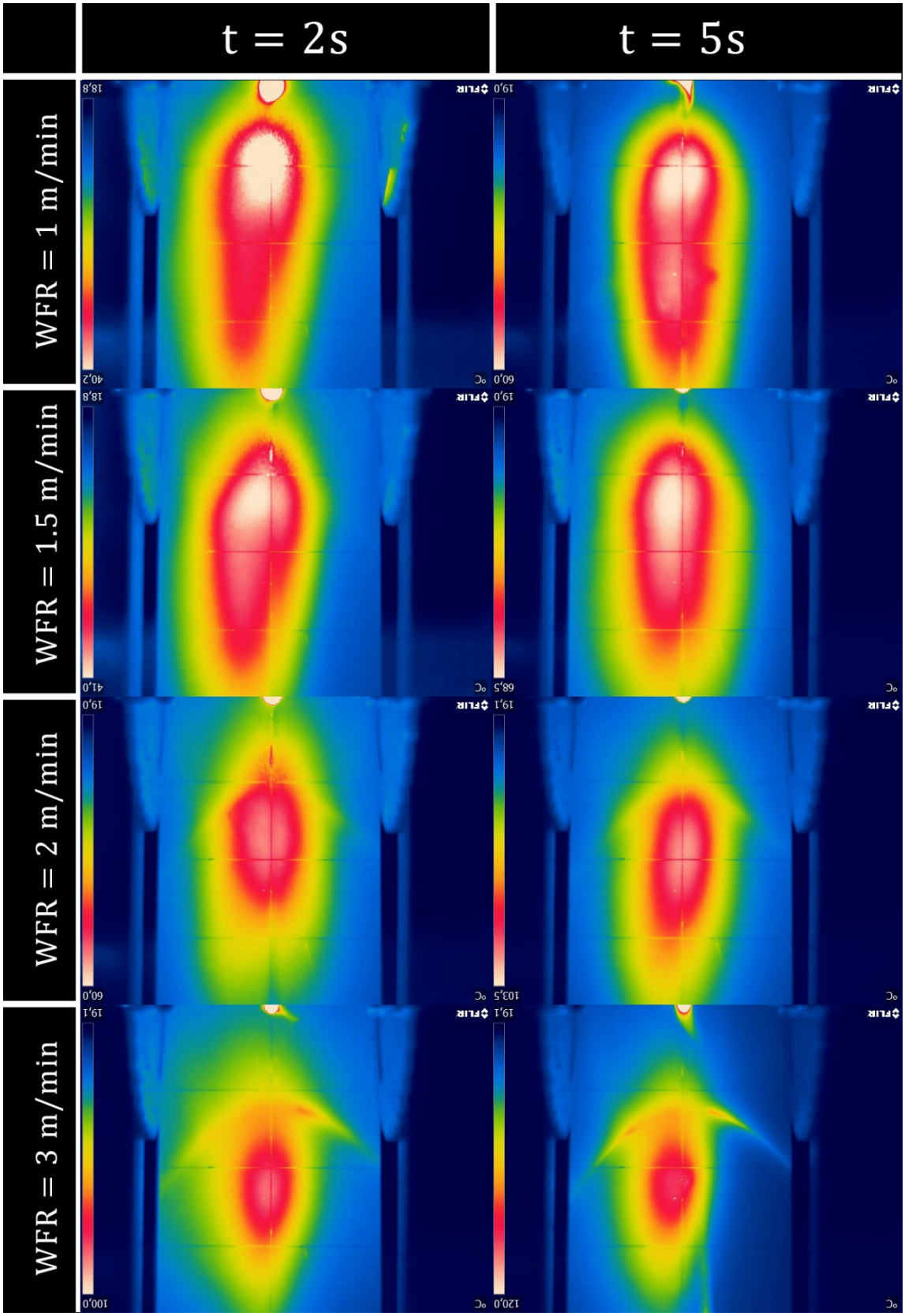

Figure 30. Thermal photos of reflected beam shapes with a different laser parameters and irradiation time.

8.2.3 Third step

Because of the limitation in size of the detection zone of power meter that was used, it was decided to find such kind of parameters that can give the smallest shape size of the reflected light. For the reason that study has to have varied laser power and the angle of the wire and, in addition, interaction time has no influence on the shape, WFR was changed for the different angles according with meanings in the table 11. Infra-red camera was used to show changes in the geometry of the shape that are shown on figure 31. From photos it can be seen that the shape of the reflected beam becomes smaller with increasing in wire speed. Because of the set-up limitations it was decided to use maximum possible WFR with the meaning of 4m/min as it gave the smallest shape of the reflected beam.

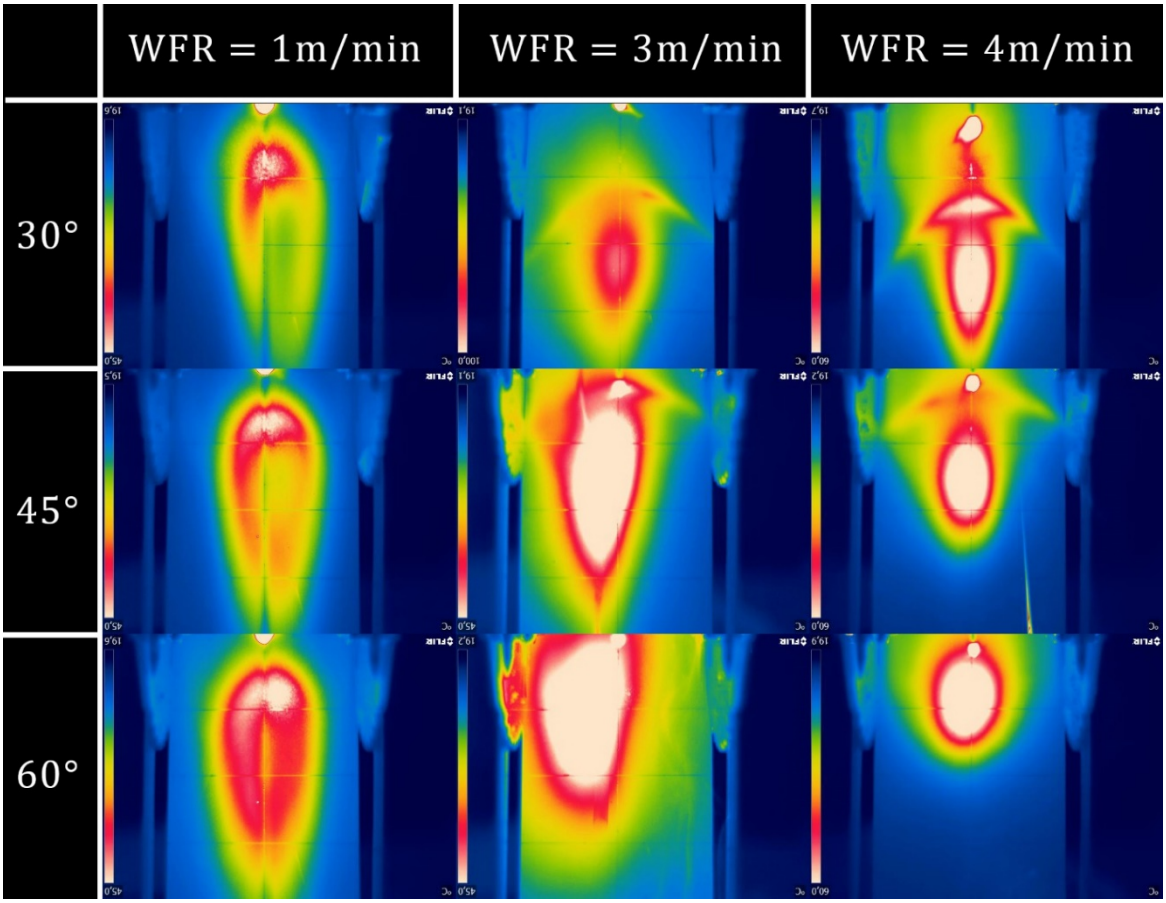

Figure 31. Thermal photos of reflected beam shapes with a different WFR and angles.

Table 11. Parameters for the third step of the experiment.

Wire angle, °	WFR, m/min	Time, s	Power, kW	Focal position, mm	Beam diameter, mm
30	1	2	2	+10	0.76
	3				
	4				
45	1				
	3				
	4				
60	1				
	3				
	4				

8.2.4 Fourth step

The next step was to find a position of the reflected beam. Black-painted plate and infra-red camera were used. The plate has a scale that gives information about position of the heated area. It was observed that this area changed the location on the vertical axis through the changes in set-up parameters. Table 12 shows parameters of the set-up which are were used. Three different angles were chosen. Reflection area was found for each parameter with various laser power and it is also shown in table 12. The step for the laser power was 100 kw when the wire was fully melted. For different angles some of the power meanings were skipped for the reason that it was assumed that the wire will not melt with this power. Tool “Grid” in the Photoshop was used to find an exact location of the reflected beam. The area of thermal photo was splinted into squares; each square has height of approximately 3.5 mm (figure 32). That meaning was found from the scale on the plate. Thermal images of the experiment are shown on figures 33, 35 and 37. Photos on figures 34, 36 and 38 show images from high-speed camera, which are help to see when the melt process starts and when the droplet becomes too unstable to do not continue the experiment.

Table 12. Parameters for the fourth step and the shape location.

Wire angle, °	Power, kW	Shape location on the vertical axe, mm	WFR, m/min	Laser interaction time, s	Focal position, mm	Beam diameter, mm
30	0.8	-	4	5	+10	0.76
	1	-				
	1.1	-				
	1.2	-				
	1.3	85-145				
	1.4	85-148				
	1.5	90-145				
	1.6	90-140				
	1.7	90-147				
	1.8	90-143				
	1.9	90-150				
	2	80-140				
	2.1	80-140				
45	1	-				
	1.1	-				
	1.2	-				
	1.3	-				
	1.4	108-173				
	1.5	106-172				
	1.6	111-170				

Table 12 continues. Parameters for the fourth step and the shape location.

Wire angle, °	Power, kW	Shape location on the vertical axe, mm	WFR, m/min	Laser interaction time, s	Focal position, mm	Beam diameter, mm
45	1.7	113-170	4	5	+10	0.76
	1.8	102-174				
	1.9	113-176				
	2	110-175				
60	1	-				
	1.2	-				
	1.3	134-178				
	1.4	130-175				
	1.5	131-180				
	1.6	131-172				
	1.7	131-171				
	1.8	132-172				
	1.9	131-175				
	2	123-178				

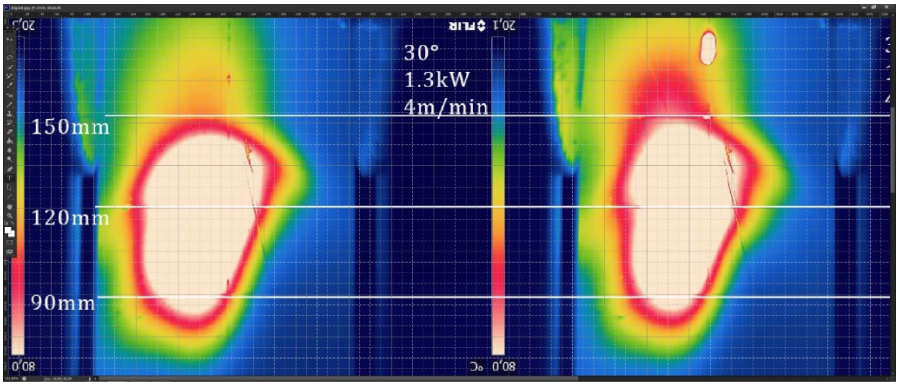

Figure 32. Screenshot from Photoshop software.

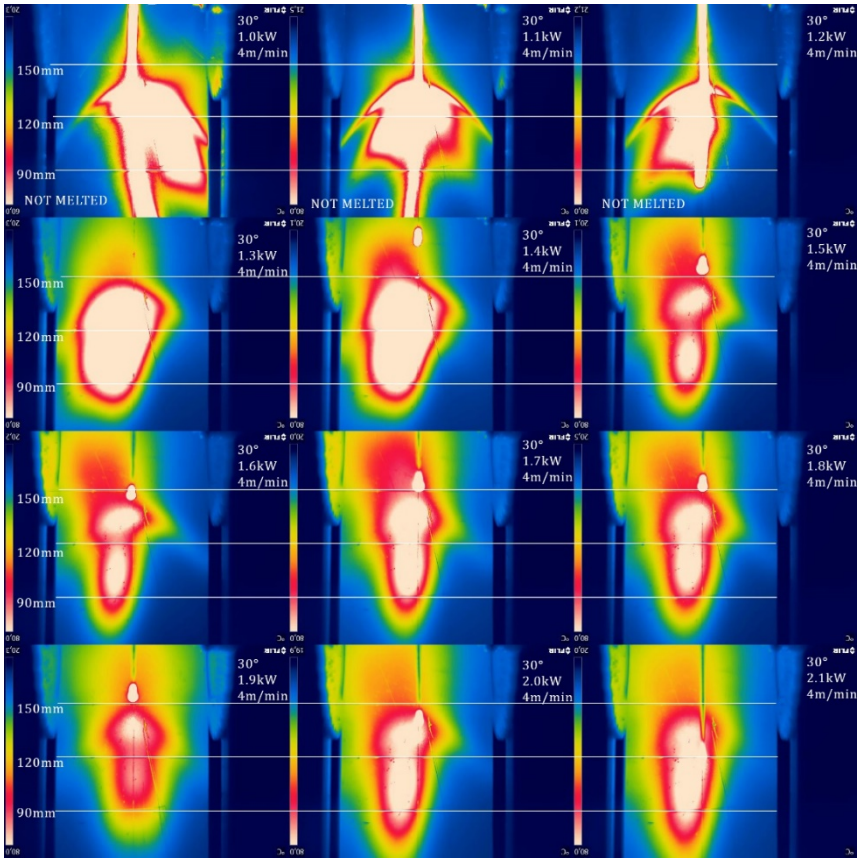

Figure 33. Thermal photos of reflected beam shapes with a different laser power using 30° angle of wire.

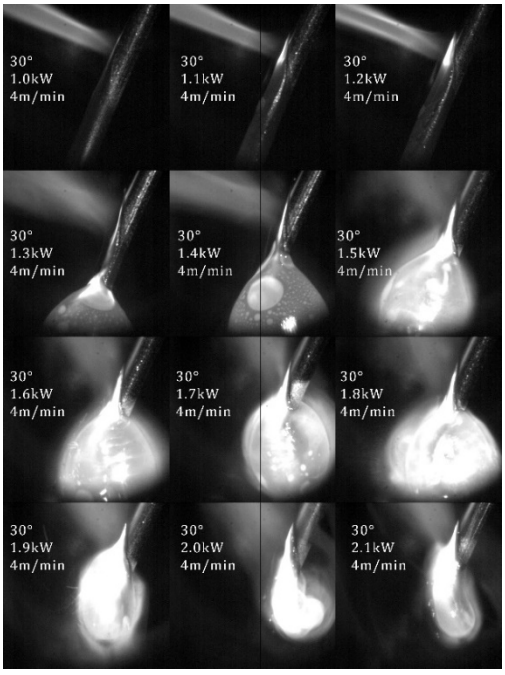

Figure 34. Thermal photos of reflected beam shapes with a different laser power using 30° angle of wire.

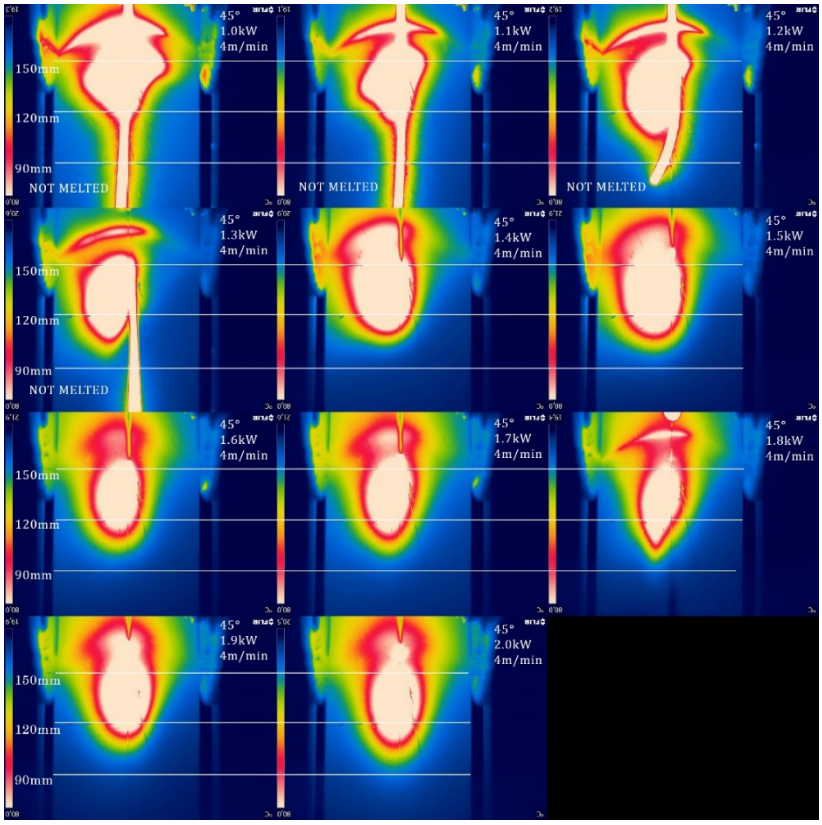

Figure 35. Thermal photos of reflected beam shapes with a different laser power using 45° angle of wire.

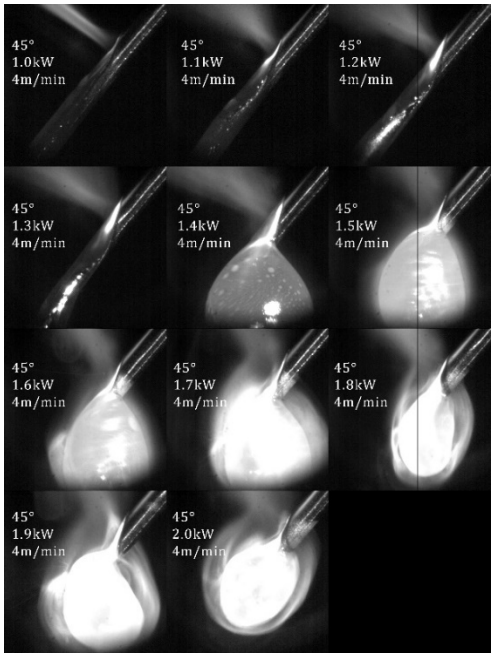

Figure 36. Thermal photos of reflected beam shapes with a different laser power using 45° angle of wire.

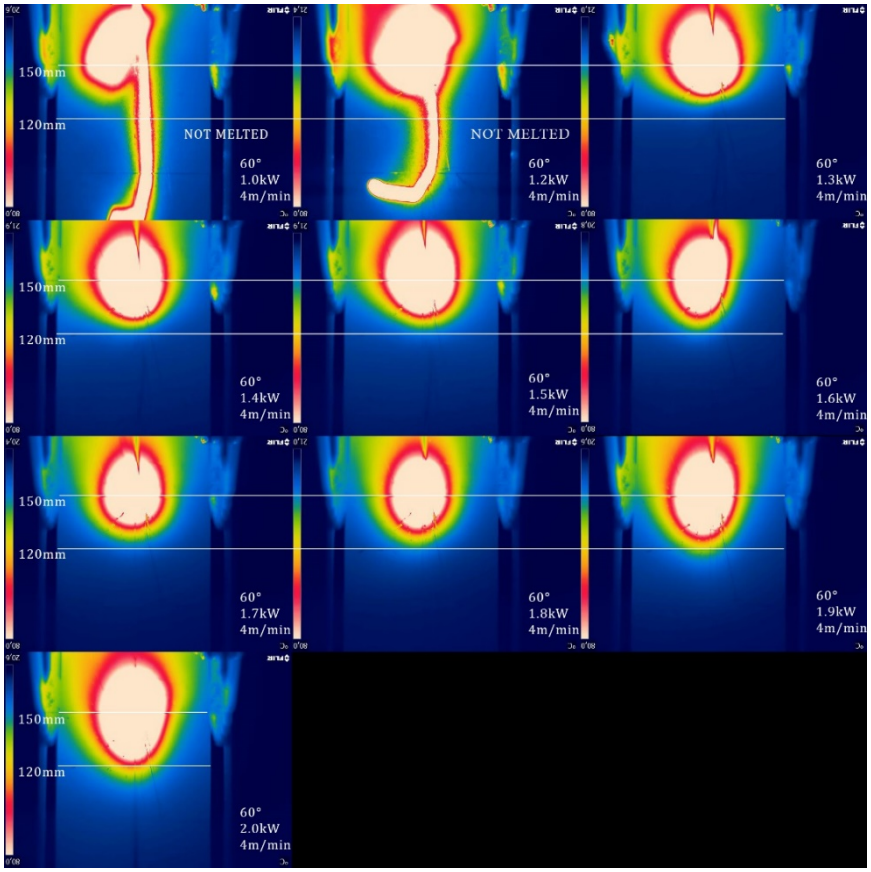

Figure 37. Thermal photos of reflected beam shapes with a different laser power using 30° angle of wire.

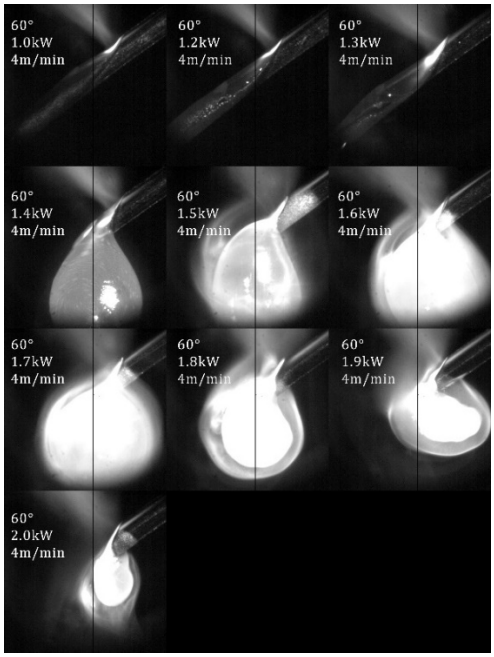

Figure 38. Thermal photos of reflected beam shapes with a different laser power using 30° angle of wire.

8.2.5 Fifth step

The last step of the study is measuring of reflection coefficient using power meter. All of set-up parameters completely the same like in table 12. New set-up parts were drawn in AutoCAD software (figure 39). Black-painted plate was replaced by the power meter (figure 40). Sensitive zone of the power meter was positioned according to the shape location from the table 12. Table 13 shows the reflection coefficient in the percentage meaning for different angles and power. figure 41 illustrated dot plots based on Table 13. Linear approximation was used to show trend line.

Table 13. Results of the fifth step.

Wire angle, °	Laser power, kW	Reflected power, kW	Reflection coefficient, %
30	1.3	0.290	22.31
	1.4	0.400	28.57
	1.5	0.383	25.53
	1.6	0.359	22.44
	1.7	0.386	22.71
	1.8	0.360	20.00
	1.9	0.394	20.74
	2.0	0.480	24.00
	2.1	0.490	24.50
45	1.4	0.320	22.86
	1.5	0.298	19.87
	1.6	0.320	20.00
	1.7	0.350	20.59
	1.8	0.330	18.33
	1.9	0.366	19.26
	2.0	0.350	17.50
60	1.3	0.315	24.23
	1.4	0.315	24.23
	1.5	0.280	22.50
	1.6	0.347	18.67
	1.7	0.271	21.68

Table 13 continues. Results of the fifth step.

Wire angle, °	Laser power, kW	Reflected power, kW	Reflection coefficient, %
60	1.8	0.300	15.94
	1.9	0.355	16.67
	2.0	0.380	18.68

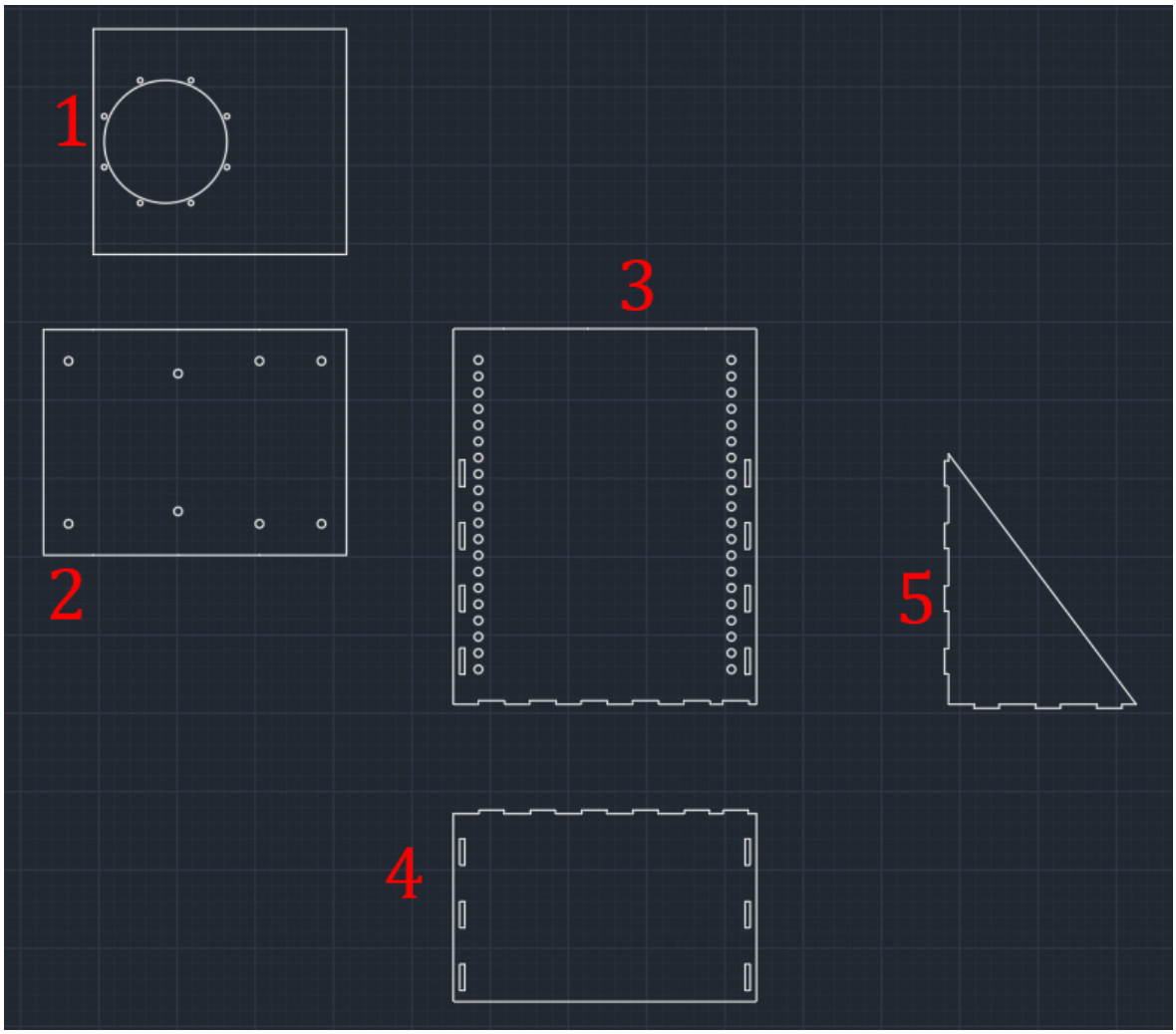

Figure 39. Drawing of new metallic parts for the set-up. 1 – Front-side protective cover plate for the power meter; 2 – Back-side fix cover plate for the power meter; 3, 4, 5 – Parts of support structure for the power meter.

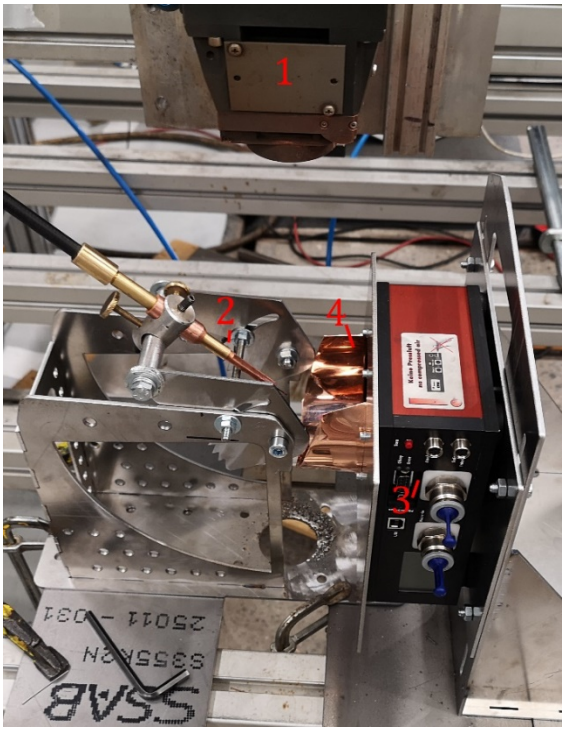

Figure 40. Set-up to measure intensity of the reflected light. 1 - laser processing head of ytterbium laser system “YLS-10000-S4”; 2 - Feed nozzle with carbon-manganese steel wire “OK Autrod 12.64”; 3 – Compact Power Monitor PRIMES CFM-F (800-1100 nm); 4 - Light catching surface nearby sensitive area.

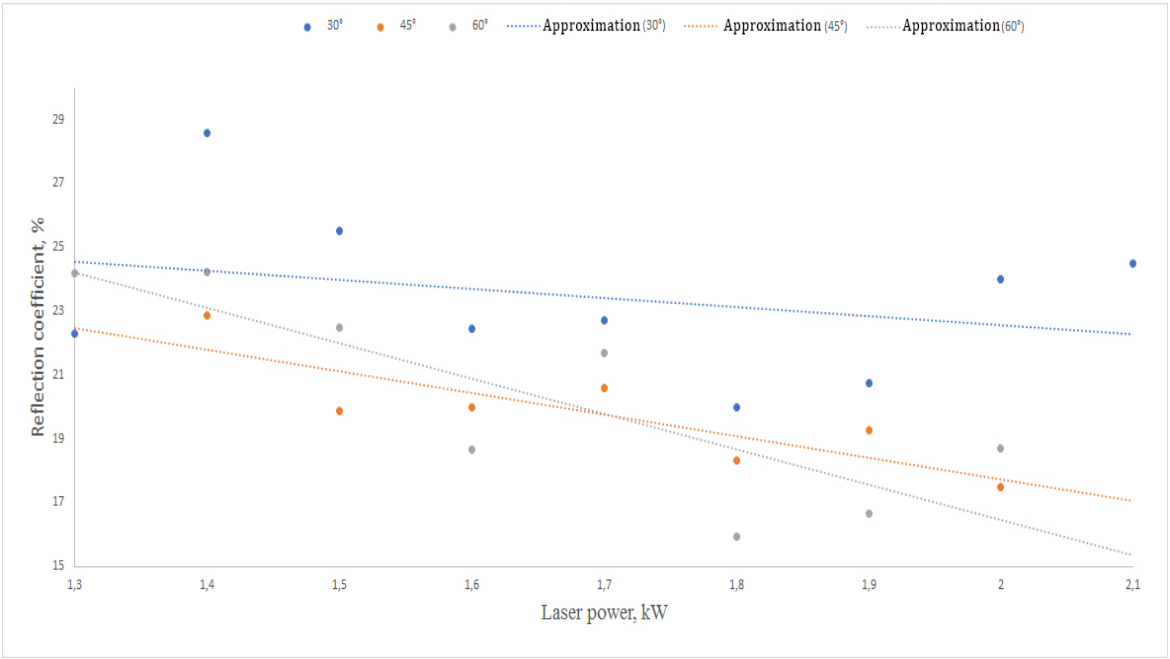

Figure 41. Dot plots illustration of the reflection coefficient with approximation lines for different wire angles and laser power.

9 RESULTS AND DISCUSSION

It can be seen from the table 9 that small beam diameter in combination with high WFR can destroy the plate for the reason that small beam size in comparing with bigger one gives higher meaning of power density. Equation 1 describes the dependence between power density q and the size of an irradiation area S, where P is a laser power, A is an absorption coefficient. Equation 2 shows the dependence between the irradiation area S and the meaning of beam diameter d:

$$q = PA / S \tag{1}$$

$$S = \pi \frac{d^2}{4} \tag{2}$$

Equitation 3, which is a transformation of equation 2 shows that power density strictly dependent on beam diameter. It is a reason why the focal position was changed and the beam diameter was increased with the aim of do not damage plate:

$$q = \frac{4PA}{\pi d^2} \tag{3}$$

Power meter, which was used in the set-up (figure 40), has sensitive area with diameter of 100 mm, so it was very important to explore if there are any significant changes in shape distribution for the same power but with different interaction time. That is why it was decided to use 2 seconds interaction time against 5 seconds due to the reason that no significant changes were observed (figure 30).

For the reason of limited time to access the laboratory, the decision about stable FWR was made to cut experimental part for this study. It was necessary to find, which of the available WFR meanings are better in case of limitation in sensitive are of the power meter. From the figure 31 it was concluded that WFR of 4 m/min leads to the smallest thermal shape of reflected beam for any of the chosen angles.

The main role of the table 12 is to show the location of the reflected beam falling and on which distance from the working table it is. It can be seen that the shape location almost unchanged with a slight increasing in laser power. However, the position of it influences significant changes with the changes in wire angle. The base law of geometrical optics can easily explain this fact.

From the results of power meter measurements, the reflection coefficient was found as the ratio of the laser power to the reflected power. It can be seen from the table 13 and figure 41 that in case of using "OK Autrod 12.64" wire 30° angle gives the biggest reflection in comparison with 45° and 60°. It can be mentioned that when power increases, reflection coefficient becomes smaller. This fact is described by the mechanism of the wire surface formation when it is melted. figure 42 shows surface of the wire using different power with the angle of 45°. It can be seen, that with 1.4 kW the wire does not fully melt in the area of laser beam and has some kind of "protrusion" in the end (green line). For this reason, light almost does not scatter inside a liquid zone of the metal and it is reflected with a bigger value in compare with 2.0 kW. Significant part of the light that can be reflected goes through the liquid metal droplet (orange zone) and experiencing scattering; part of the scattered photons goes with almost the same direction like the laser beam, which is reflected from the wire. However, most of them scattered in other directions, especially in the direction to the base metal. If compare reflection coefficient for 1.4 kW and 2.0 kW power in case 45° angle (table 13), it loses approximately 24% of overall reflection. With power increasing, reflection has to become lower. Based on the geometrical optics, it is suggested that red zones on figure 42 shows approximately directions of the reflected light, that is come from the laser head, which is above the wire. This assumption explains why the reflected zone in case of 1.4 kW looks more spherical than the zone of 2.0 kW (figure 43).

Graphs on figure 41 shows dependences between power and reflection coefficient for angles of 45° and 60°. The linear approximations of them looks the same like in Salminen`s research [1], but they have inverse meanings in comparison with graphs that he got (figure 44). It can be explained by the figure 45. There are shown two scenarios, when the laser beam area fully fall into the wire surface and when it is not fall on it. Picture A described Salminen`s approach, picture B described approach of this study. Salminen used constant power of 5 kW and started from low WFR then moving to bigger meanings. It leads to the fact, that with

increasing in WFR, wire has no more time to melt with the same speed for the reason that wire volume that has to be melted is increased. The opposite approach is used in this study. That is why graphs look like inverse to each other.

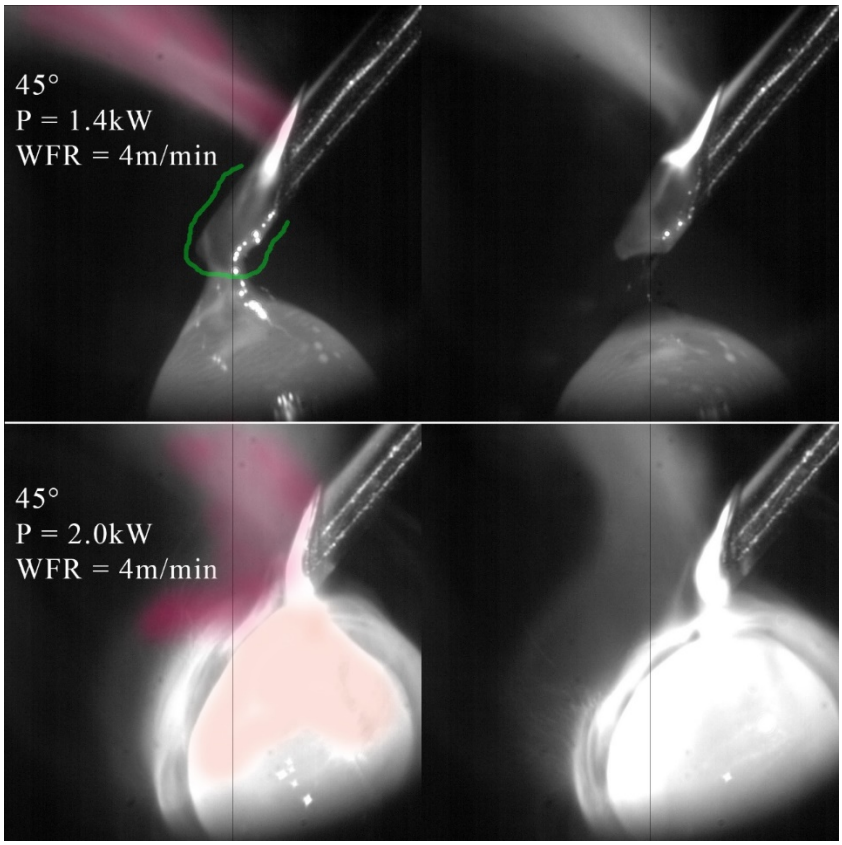

Figure 42. Photos of different conditions of the wire for 1.4 kW and 2.0 kW with constant WFR using angle of 45°. Green line - "protrusion" in the end of the wire; red zone – possible directions of the reflected beam; orange zone – light scattering.

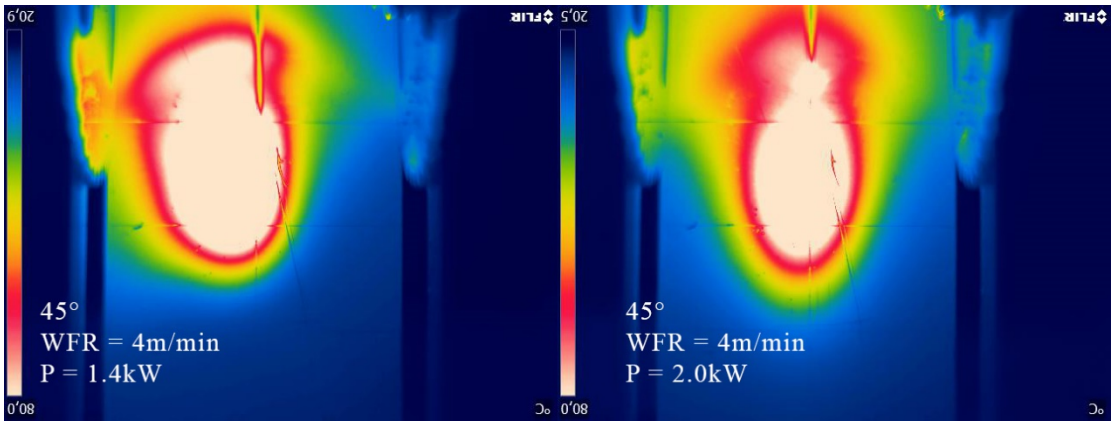

Figure 43. Thermal photo of the beam shapes for 1.4 kW and 2.0 kW with constant WFR using angle of 45°.

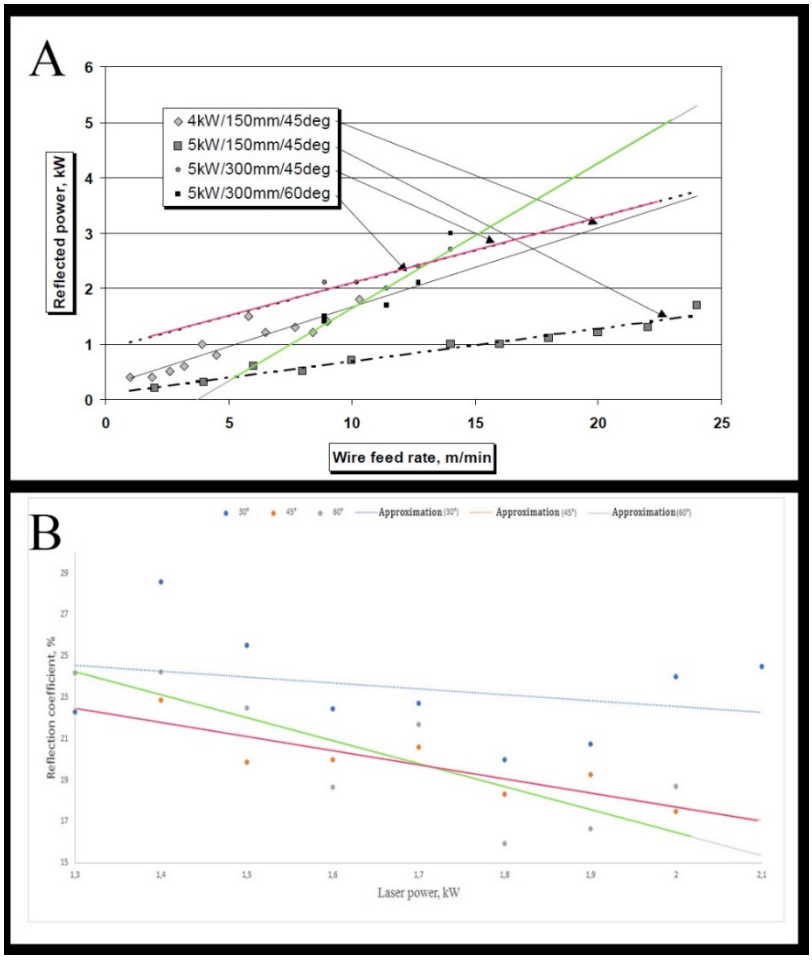

Figure 44. Comparison of two graphs. A – Salminen's results [1]; B – Figure 41. Green line – approximation for 60°; Red line – approximation for 45°.

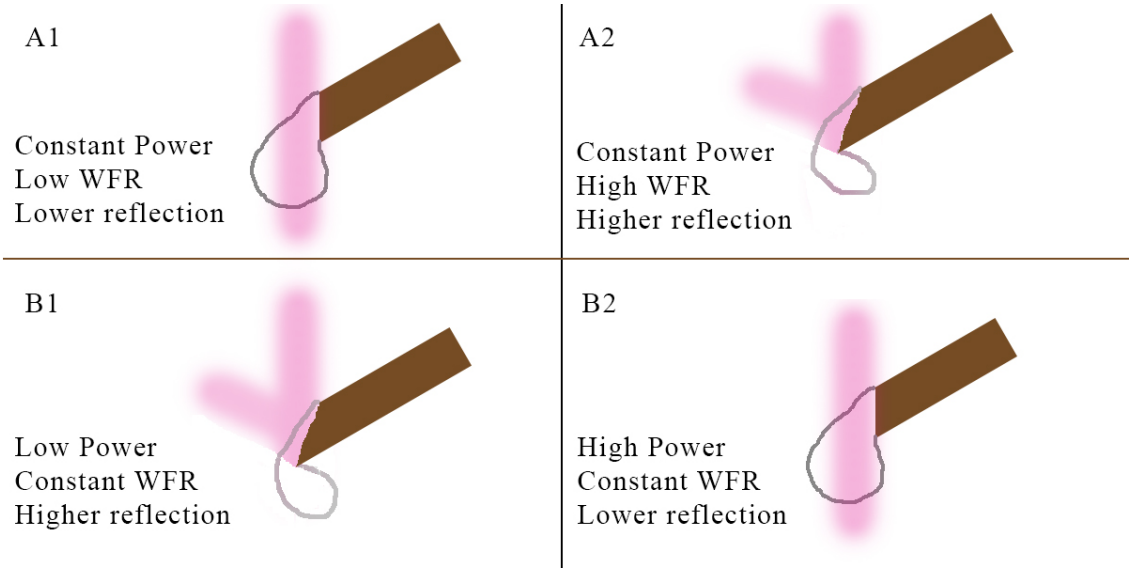

Figure 45. Illustration of different experimental approaches. A1, A2 - Salminen's approach; B1, B2 – the approach of this study.

10 SUMMARY

The approach to measuring reflection coefficient was developed in the study. It was found that interaction time has no influence on the character of the reflection. According to the thermal photos from figure 31 it can be concluded, that reflection is growing when WFR is increasing. With a constant WFR and the angle, the reflection coefficient is decreased with increasing in power. This correlation has linear character. Wire angle has significant influence on the reflection.

For the reason that all of the results are proofed by comparison with Salminen's results [1] and by analysis of high-speed and thermal images (figures 42, 43), it can be concluded that the wire surface has one of the major influence on the reflection coefficient in case of using constant laser-wire combination. WFR and laser power have influence on changes in the geometry of wire surface, but have no influence on the reflection by themselves. It is suggested that for different wire and laser combination the results will not be the same due to the different absorption coefficient.

Based on the results, it can be offered to future studies to go deeper into the sphere of droplet and wire monitoring throughout the melting process following the example of study done by Shao, Wang, and Zhang [43]. The research was successful, all targets were achieved, and the results were analyzed. Analytical approach of results was applied and conclusions were done.

LIST OF REFERENCES

1. Salminen A. The effects of filler wire feed on the efficiency, parameters and tolerances of laser welding. Lappeenranta: Lappeenranta University of Technology, 2001. 82 p.
2. Arata Y. et al. High Power CO2 Laser Welding of Thick Plate - Multipass Weding with Filler Wire // Weld. Res. Inst. Osaka Univ. 1986. Vol. 15. P. 27–34.
3. Katayama S. 1 - Introduction: fundamentals of laser welding // Handbook of Laser Welding Technologies / ed. Katayama S. Woodhead Publishing, 2013. P. 3–16.
4. Sakamoto H., Iwase T., Shibata K. The effect of twin spot beam arrangement on energy coupling during welding. Study of twin spot Nd: YAG laser welding of aluminium alloys // Weld. Int. 2004. Vol. 18, № 9. P. 677–682.
5. Miyashita Y. 16 - Developments in twin-beam laser welding technology // Handbook of Laser Welding Technologies / ed. Katayama S. Woodhead Publishing, 2013. P. 465.
6. Karhu M. et al. Comparison of laser welding methods in position welding of edge joint of austenitic stainless steel // Proceedings of the 14th Nordic Laser Materials Processing Conference NOLAMP. 2013. Vol. 14. P. 26–28.
7. Moon J.H. et al. Melting characteristics of metals by combined laser beams with different wavelengths // J. Laser Appl. 2003. Vol. 15, № 1. P. 37–42.
8. Shibata K., Iwase T., Sakamoto H. Effect of twin spot beam configuration on overlap joints welding - Study of twin spot Nd: YAG laser welding of aluminum alloys (rep. 2) // Yosetsu Gakkai Ronbunshu/Quarterly J. Japan Weld. Soc. 2003. Vol. 21, № 2. P. 213–218.
9. Ohashi R. et al. Extension of gap tolerance in square butt joint welding with Nd:YAG laser // Weld. Int. 2004. Vol. 18, № 1. P. 16–23.
10. Tsukamoto T., Kawanaka H., Maeda Y. Laser narrow gap welding of thick carbon steels using high brightness laser with beam oscillation // 30th International Congress on Applications of Lasers and Electro-Optics, ICALEO 2011. 2011. P. 141–146.
11. Zhang X. Developments in multi-pass laser welding technology with filler wire // Handbook of Laser Welding Technologies. 2013. P. 459–477.
12. Mahrle A., Beyer E. Heat sources of hybrid laser-arc welding processes // Hybrid

Laser-Arc Welding. 2009. P. 47–84.

13. Olsen F.O., Olsen F.O. Hybrid laser-arc welding // Woodhead Publishing in materials. Cambridge, U.K. : Boca Raton, Fla.: Woodhead Pub. ; CRC Press, 2009. 323 p.
14. Katayama S. Fundamentals of hybrid laser-arc welding // Hybrid Laser-Arc Welding. 2009. P. 28–46.
15. Lippert R.B., Lachmayer R. A Design Method for SLM-Parts Using Internal Structures in an Extended Design Space BT - Industrializing Additive Manufacturing - Proceedings of Additive Manufacturing in Products and Applications - AMPA2017 / ed. Meboldt M., Klahn C. Cham: Springer International Publishing, 2018. P. 14–23.
16. 3Diligent Corporation. Directed Energy Deposition [Electronic resource]. 2019. URL: https://www.3diligent.com/3d-printing-service/directed-energy-deposition/ (accessed: 09.04.2019).
17. DebRoy T. et al. Additive manufacturing of metallic components – Process, structure and properties // Prog. Mater. Sci. 2018. Vol. 92. P. 112–224.
18. Kim J.-D., Peng Y. Plunging method for Nd:YAG laser cladding with wire feeding // Opt. Lasers Eng. 2000. Vol. 33, № 4. P. 299–309.
19. Brandl E. et al. Deposition of Ti-6Al-4V using laser and wire, part II: Hardness and dimensions of single beads // Surf. Coatings Technol. 2011. Vol. 206, № 6. P. 1130–1141.
20. Schmidt M., Otto A., Kägeler C. Analysis of YAG laser lap-welding of zinc coated steel sheets // CIRP Ann. - Manuf. Technol. 2008. Vol. 57, № 1. P. 213–216.
21. Seto N., Katayama S., Matsunawa A. High-speed simultaneous observation of plasma and keyhole behavior during high power CO2 laser welding: Effect of shielding gas on porosity formation // J. Laser Appl. 2000. Vol. 12, № 6. P. 245–250.
22. Lee S.-J. et al. Weldability and keyhole behavior of Zn-coated steel in remote welding using disk laser with scanner head // J. Laser Appl. 2013. Vol. 25, № 3.
23. Zhang M.J. et al. Observation of spatter formation mechanisms in high-power fiber laser welding of thick plate // Appl. Surf. Sci. 2013. Vol. 280. P. 868–875.
24. Mizutani M., Katayama S. Keyhole behavior and pressure distribution during laser irradiation on molten metal // ICALEO 2003 - 22nd International Congress on Applications of Laser and Electro-Optics, Congress Proceedings. 2003.
25. Matsunawa A. et al. Experimental and theoretical studies on keyhole dynamics in laser welding // ICALEO. Laser Institute of America, 1996. Vol. 1996, № 1. P. 67.

26. Otto A. et al. Numerical simulations- A versatile approach for better understanding dynamics in laser material processing // Physics Procedia. 2011. Vol. 12, № PART 1. P. 11–20.
27. Fabbro R. Limiting process for keyhole propagation during deep penetration laser welding // Proceeding of 5th international congress on laser advanced materials processing (LAMP). 2009.
28. Seto N., Katayama S., Matsunawa A. Porosity formation mechanism and suppression procedure in laser welding of aluminium alloys // Weld. Int. 2001. Vol. 15, № 3. P. 191–202.
29. Börner C. et al. Influence of ambient pressure on spattering and weld seam quality in laser beam welding with the solid-state laser // 30th International Congress on Applications of Lasers and Electro-Optics, ICALEO 2011. 2011. P. 621–629.
30. Kägeler C., Schmidt M. Frequency-based analysis of weld pool dynamics and keyhole oscillations at laser beam welding of galvanized steel sheets // Physics Procedia. 2010. Vol. 5, № PART 2. P. 447–453.
31. Solana P., Ocaña J.L. A mathematical model for penetration laser welding as a free-boundary problem // J. Phys. D. Appl. Phys. 1997. Vol. 30, № 9. P. 1300–1313.
32. Andrews J.G., Atthey D.R. Hydrodynamic limit to penetration of a material by a high-power beam // J. Phys. D. Appl. Phys. 1976. Vol. 9, № 15. P. 2181–2194.
33. Sensortherm GmbH. Digital High-Speed Pyrometers for Laser Power Control [Electronic resource]. 2018. URL: https://www.sensortherm.de/userfiles/file/datenblaetter/application/Sensortherm-Application_LaserPowerControl.pdf (accessed: 14.04.2019).
34. Rodriguez N. et al. Wire and arc additive manufacturing: a comparison between CMT and TopTIG processes applied to stainless steel // Weld. World. 2018. Vol. 62, № 5. P. 1083–1096.
35. Kisielewicz A. et al. Spectroscopic monitoring of laser blown powder directed energy deposition of Alloy 718 // Procedia Manufacturing. 2018. Vol. 25. P. 418–425.
36. Mukherjee T. et al. Printability of alloys for additive manufacturing // Sci. Rep. 2016. Vol. 6.
37. Katayama S. Defect formation mechanisms and preventive procedures in laser welding // Handbook of Laser Welding Technologies. 2013. P. 332–373.
38. Terrassa K.L. et al. Reuse of powder feedstock for directed energy deposition //

Powder Technol. 2018. Vol. 338. P. 819–829.

39. GRAINGER. The New 2019 Grainger Catalog [Electronic resource]. URL: https://www.grainger.com/content/general-catalog (accessed: 16.04.2018).
40. Sciaky inc. Advantages of Wire AM vs. Powder AM [Electronic resource]. URL: http://www.sciaky.com/additive-manufacturing/wire-am-vs-powder-am (accessed: 16.04.2019).
41. ESAB. OK AUTROD 12.64 [Electronic resource]. URL: https://www.esabna.com/gb/en/products/filler-metals/mig-mag-wires-gmaw/mild-steel-wires/ok-autrod-12-64.cfm (accessed: 14.05.2019).
42. IPG Laser GmbH. Operating Manual Ytterbium Laser System YLS-10000-S4 S/N 11066750. 2011. 232 p.
43. Shao Y., Wang Z., Zhang Y. Monitoring of liquid droplets in laser-enhanced GMAW // Int. J. Adv. Manuf. Technol. 2011. Vol. 57, № 1–4. P. 203–214.